

Cities

Innovative framework for identification and spatiotemporal dynamics analysis of industrial land at parcel scale with multidimensional attributes

--Manuscript Draft--

Manuscript Number:	JCIT-D-24-02243
Article Type:	Full Length Article
Section/Category:	Full Length Article
Keywords:	Industrial land; Land parcel identification; Spatiotemporal dynamics; Multidimensional framework; Multi-source data
Corresponding Author:	Zhengfeng Zhang Renmin University of China Beijing, China
First Author:	Weilong Kong
Order of Authors:	Weilong Kong Jing Huang Lu Niu Shuocun Chen Jiahe Zhou Zhengfeng Zhang
Manuscript Region of Origin:	Asia Pacific
Abstract:	Understanding the spatiotemporal dynamics of industrial land is crucial for sustainable land use and industrial transformation. However, data and methodological limitations hamper extensive, long-term studies of industrial land from a perspective of high granularity and multiple dimensions. This study develops a methodological framework employing multi-source data to identify industrial land and its multidimensional attributes at the parcel scale, enabling systematic analysis of external attributes (including quantity scale and spatial pattern) and internal attributes (including functional structure and utilization intensity). The framework's validity is demonstrated through a case study of the Southern Jiangsu Urban Agglomeration in China from 1990 to 2020. The industrial land identification achieves an overall accuracy of 94.70% , with temporal discrimination accuracy of 82.63%. Detailed insights into parcel morphology support a comprehensive three-decade analysis across urban-rural areas, revealing a twentyfold increase in industrial land area. Attribute transformation speed exhibits an "inverted U-shaped" change, with internal attributes lagging behind external ones by about five years. Moreover, the study reveals significant correlations among the attributes, as well as a spatially heterogeneous evolution influenced by economic and policy factors. The study contributes theoretically by developing an innovative tool and practically by supporting refined management and monitoring of industrial land.
Suggested Reviewers:	Weixin Ou Professor, Nanjing Agricultural University owx@njau.edu.cn Professor Ou is an expert in the field of land system science, and has long been engaged in the research of land sustainable use and urban planning. Jeong-II Park Keimyung University jip@kmu.ac.kr Jeong-II Park is a researcher in the field of industrial land, engaged in industrial land use and management research.

Dear Editor of *Cities*,

We are pleased to submit our manuscript titled "*Innovative framework for identification and spatiotemporal dynamics analysis of industrial land at parcel scale with multidimensional attributes*" for consideration in *Cities*. This letter highlights the core contributions of our study, which are closely aligned with the thematic scope of your esteemed journal.

Our study addresses the critical need for understanding the spatiotemporal dynamics of industrial land, essential for optimizing spatial governance and advancing industrial transformation. Despite the significance of this issue, the scarcity of granular, multi-dimensional data has historically impeded comprehensive studies. In response, our manuscript introduces an innovative methodology employing multi-source data to accurately identify industrial land parcels across long time series. Additionally, we have developed a robust multidimensional analytical framework that assesses both external (quantitative scale and spatial patterns) and internal (functional structure and utilization intensity) attributes of industrial land. The framework has been effectively applied to the Southern Jiangsu Urban Agglomeration in China from 1990 to 2020, demonstrating its practicality and effectiveness.

Key findings from our study include:

- 1) Exceptional accuracy in industrial land identification, with overall accuracy reaching 94.70% and temporal discrimination accuracy at 82.63%. Detailed expressions of parcel morphology (boundaries, area, etc.) are meticulously highlighted.
- 2) The framework conducts long-term analyses spanning 30 years, covering both urban and rural areas on the spatial scale.
- 3) Industrial land expanded more than twentyfold during the study period. The transformation speed of various dimensional attributes exhibited an "inverted U-

shaped" change, with internal attributes lagging behind external attributes by approximately five years.

- 4) Significant correlations among the attributes of industrial land are uncovered, and a spatially heterogeneous evolutionary process driven by economic and policy factors is highlighted.

The methodological innovations and the depth of our analysis provide invaluable insights into the spatiotemporal dynamics of industrial land use. This work not only enriches the academic discourse but also equips policymakers and urban planners with actionable tools. We are confident that our findings will significantly captivate your readers and contribute to advancing the field of urban planning and sustainable development.

Thank you for considering our manuscript. We eagerly anticipate your response.

Sincerely,

Zhengfeng Zhang

Department of Land Management, School of Public Administration and Policy

Renmin University of China

Email: zhangzhengfeng@ruc.edu.cn

Highlights

- Industrial land identification accuracy reaches 94.70%, with temporal accuracy at 82.63%.
- Parcel morphology, including boundaries and area, is accurately depicted.
- The analysis framework spans two levels and four dimensions of industrial land attributes.
- Industrial land in the study area grew by more than twentyfold from 1990 to 2020.
- The transformation pace of each attribute follows an inverted U-shaped pattern.

Innovative framework for identification and spatiotemporal dynamics analysis of industrial land at parcel scale with multidimensional attributes

Abstract: Understanding the spatiotemporal dynamics of industrial land is crucial for sustainable land use and industrial transformation. However, data and methodological limitations hamper extensive, long-term studies of industrial land from a perspective of high granularity and multiple dimensions. This study develops a methodological framework employing multi-source data to identify industrial land and its multidimensional attributes at the parcel scale, enabling systematic analysis of external attributes (including quantity scale and spatial pattern) and internal attributes (including functional structure and utilization intensity). The framework's validity is demonstrated through a case study of the Southern Jiangsu Urban Agglomeration in China from 1990 to 2020. The industrial land identification achieves an overall accuracy of 94.70%, with temporal discrimination accuracy of 82.63%. Detailed insights into parcel morphology support a comprehensive three-decade analysis across urban-rural areas, revealing a twentyfold increase in industrial land area. Attribute transformation speed exhibits an "inverted U-shaped" change, with internal attributes lagging behind external ones by about five years. Moreover, the study reveals significant correlations among the attributes, as well as a spatially heterogeneous evolution influenced by economic and policy factors. The study contributes theoretically by developing an innovative tool and practically by supporting refined management and monitoring of industrial land.

Keywords: Industrial land; Land parcel identification; Spatiotemporal dynamics; Multidimensional framework; Multi-source data

1. Introduction

Industrial land serves as a crucial spatial foundation for economic and social activities, underpinning global manufacturing development and acting as a significant source of carbon emissions and various environmental issues (Kuang et al., 2016; Chen et al., 2019). Consequently, in regional land use and management, industrial land consistently holds a prominent position (Park & Kim, 2022; Tian et al., 2015). Whether in developed or developing countries, the utilization of industrial land is continuously evolving and remains closely linked to the industrialization process (Tan et al., 2024; Yue et al., 2022). An understanding of the multidimensional characteristics of industrial land use, coupled with insights into its spatiotemporal dynamics, facilitates the adjustment of land policies and the optimization of land use in practical applications. This knowledge is also essential for grasping the causal relationships between industrial land use and other socioeconomic and environmental factors (Dai et al., 2022; Li et al., 2019). Thus, the topic has sparked widespread interest across disciplines such as land use, urban planning, geography, and public policy (Song et al., 2020; Xiong et al., 2020).

Previous studies have explored various aspects of industrial land development, including patterns of scale expansion (Kuang et al., 2016; Park & Kim, 2022), landscape morphological evolution (Zhu et al., 2019), spatial differentiation (Xie et al., 2018; Zhang et al., 2019), formation mechanisms (Zhu et al., 2018; Jiang et al., 2017), and utilization transformation (Xu & Zhang, 2021). These studies suggest that the evolution of regional industrial land significantly drives economic growth. A comprehensive understanding of the multidimensional spatiotemporal dynamics of industrial land provides insights for guiding future local

development pathways (Qiao et al., 2019; Xu & Zhang, 2021). However, despite these exploratory contributions to the theme, a deeper understanding remains relatively limited. Firstly, most studies do not feature a systematic analytical framework. They tend to analyze only a single dimension, struggle to interpret dynamics from a multidimensional perspective, and rarely uncover correlations between various attributes (Xiong et al., 2020; Zhu et al., 2019). Secondly, there is a shortage of more finely grained analysis, particularly at the parcel scale, resulting in overlooking of internal spatial forms, functional structures, and utilization intensity within industrial land (Zhang et al., 2019). Analyzing these internal attributes is crucial for revealing the patterns of industrial land transformation and potential for renovation and upgrading (Huang et al., 2022b; Long, 2022). Lastly, most studies are confined to smaller study areas and shorter periods, limiting the general applicability of the findings (Zhu et al., 2018; Gao et al., 2021).

The aforementioned research difficulties stem mainly from challenges in collecting relevant data, which diminish the feasibility of conducting in-depth studies. Many countries and regions have not established comprehensive databases containing multidimensional information on industrial land. Even basic spatial data on industrial land often lacks continuity and comparability, complicating its application in extensive, long-term studies.

In recent years, geospatial big data has been widely explored (Liang et al., 2023; Yang et al., 2023), encompassing very high-resolution (VHR) remote sensing imagery (Mao et al., 2022; Luo et al., 2019), POI data (Qin et al., 2022; Zhang et al., 2017), mobile phone signaling data (Ilieva et al., 2018; Ponce-Lopez et al., 2021), public transit usage data (Yap et al., 2018; Zhai

et al., 2019), and street view data (Fang et al., 2022; Li et al., 2017). Researchers specializing in remote sensing and geographic information science have employed these data to develop technologies such as Mapping Urban Functional Zones (MUFZ) (Nie et al., 2022; Niu et al., 2023), offering new perspectives for industrial land research.

Some studies have applied MUFZ for the identification and information extraction of industrial land (Huang et al., 2022b; Xiong et al., 2020; Xu et al., 2021), contributing positively in terms of data sources and research methods compared to traditional studies. However, it is crucial to recognize that directly applying these methods to industrial land research presents significant drawbacks: (1) They offer a lower accuracy for identifying relevant information about industrial land. Although MUFZ achieves high accuracy in identifying land uses like residential areas, commercial zones, and parks, its accuracy for industrial land is often more than 15% lower compared to these uses. (Qin et al., 2022; Huang et al., 2022a; Zhang et al., 2020); (2) The generation of analysis unit is relatively coarse. MUFZ focuses on visualizing all land use functions within urban built-up areas, generally using Traffic Analysis Zone (TAZ) or kilometer grid as analysis unit (Wu et al., 2023). However, these units are too large and their shape and area significantly differ from actual parcel boundaries, making them unsuitable for detailed analysis of specific types of land (Zhong et al., 2020); (3) MUFZ is still not applicable for long-term series studies. MUFZ heavily relies on POI data, which has been accumulated and utilized mainly in recent years. This reliance makes it almost impossible to obtain data prior to 2010 for research purposes (Zhang et al., 2022). As a result, most existing methods are designed for analyses of individual years (Qin et al., 2022; Qiao et al., 2019).

Considering the current deficiencies in the multidimensional spatiotemporal dynamics analysis of industrial land and the limitations imposed by the research data, this paper aims to propose a comprehensive research framework based on multi-source data. We develop a complete technical pathway for batch identification of multi-attribute information on industrial land parcels over long time series, complemented by an analytical framework for conducting multidimensional spatiotemporal dynamics studies using the refined data. Then we apply this framework to a case study of the Southern Jiangsu Urban Agglomeration in China from 1990 to 2020 to assess their effectiveness.

Compared to previous research, this study introduces the following innovations and contributions:

(1) We innovate the technical pathway for identifying industrial land parcels and obtaining multidimensional information based on multi-source data. In comparison to recent studies, this research yields some advancements, including: 1) Significant improvements in overall accuracy, producer's accuracy, and user's accuracy; 2) A shift from TAZ to land parcel as analysis unit, enhancing the granularity of the study; 3) An expansion from single-year to long-term series studies on the temporal scale, while covering both urban and rural areas on the spatial scale.

(2) We propose a systematic analysis framework for the multidimensional spatiotemporal dynamics of industrial land, transitioning from a single perspective to a multidimensional one. The analysis framework covers two levels (internal, external) and four dimensions (quantity scale, spatial pattern, functional structure, utilization intensity) of industrial land use,

systematically revealing the spatiotemporal dynamics of industrial land and the correlations between different attributes.

The technical pathway developed in this study enables the identification of industrial land in large-scale study areas over long time series. It meets the demands for obtaining multi-attribute information on industrial land required in related research and facilitating in the monitoring of industrial land use in practice. Additionally, this paper constructs a multidimensional spatiotemporal dynamic analysis framework for industrial land, which is not only applicable to this case area but can also be transferred to other study areas to provide an analytical tool. This significantly aids in systematically revealing the patterns and evolutionary rules of industrial land use.

Following the introduction, the structure of the paper is as follows: Section 2 describes the study area, data, and methods. Then, Section 3 presents the results of industrial land parcel identification, accuracy verification, and multidimensional spatiotemporal dynamics analysis. Finally, Section 4 discusses the insights and Section 5 concludes.

2. Data and Methods

2.1 Study area

The Southern Jiangsu Urban Agglomeration, located in the Yangtze River Delta region, consists of five cities: Nanjing, Zhenjiang, Suzhou, Wuxi, and Changzhou. It encompasses 41 districts and counties, with a total area of 28,096.34 km² (Fig.1). As of 2020, the population reached 38.01million, with an urbanization rate of 80.66%, which is approximately 17% higher than the national average. The per capita GDP was 156,200 yuan, approximately 1.5 times the national average, with the industrial sector contributing 7.34% of the national total. This makes the Southern Jiangsu Urban Agglomeration a microcosm of China's rapid industrialization and urbanization (Gu et al., 2024), establishing it as a highly representative case study area.

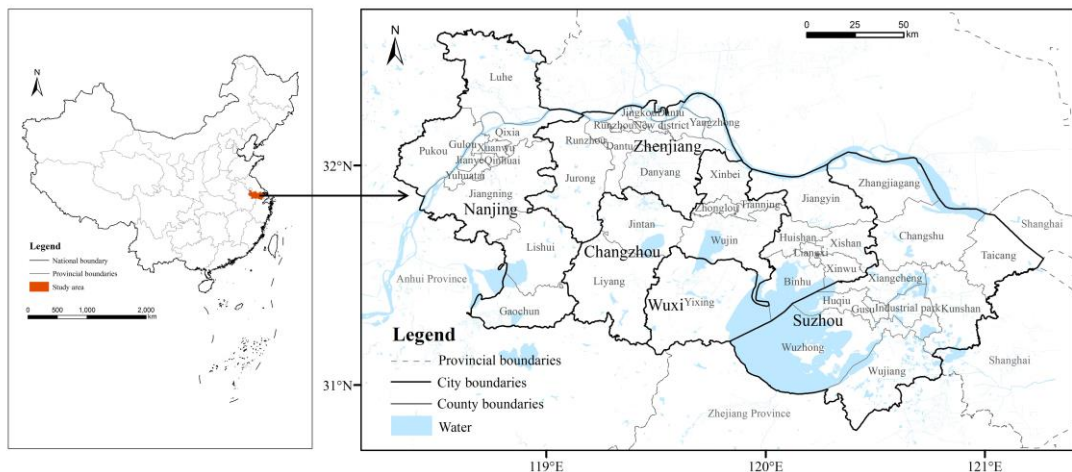


Fig.1. Study area

2.2 Data sources and preprocessing

This study employs multi-source data, incorporating five types: remote sensing images, land cover, Points of Interest (POI), road and water system information, and building information (Appendix A).

First, high-resolution remote sensing imagery from Landsat is employed to calculate

ground texture characteristics.

Second, the land cover data is sourced from six distinct providers. Sources ①-⑤ offer high resolutions of either 10m or 1m, providing the fine spatial details essential for generating base maps of construction land. Source ⑥ offers a longer temporal scale, which is crucial for determining the formation years of parcels.

Road and water system data are sourced from Open Street Map (OSM), which offers free access to multi-level road networks and hydrographic vector data. This study utilizes this data for delineating construction land parcels. To ensure reasonable parcel segmentation, we reference related research (Xu et al., 2021; Wu et al., 2023) and conduct repeated experiments within the study area. Ultimately, motorways, primary, secondary, tertiary, and trunk roads, along with all water networks from OSM, are extracted to serve as the basis for parcel segmentation. Overly detailed linear features such as footways and living streets are excluded to maintain focus on relevant geographical data.

POI data, which includes spatial location and provides abundant attribute information such as names, addresses, and types, is extensively used in this study. To ensure data completeness, we incorporate POIs obtained from Amap and NavInfo, two platforms in China. Amap is one of the China's most widely used navigation platforms, and NavInfo is the first company authorized by the government for the commercial development of electronic navigation maps in China. These platforms have accumulated a massive amount of POI data with rapid update speeds. Errors and duplicate records in the original data are cleaned up, and POIs irrelevant to the study's goals, such as "public toilets" and "bus stations," are excluded,

resulting in 1,577,987 records for research use. Additionally, since the POI data's classification system does not categorize industrial enterprises separately, a reclassification is necessary. Initially, by referencing the "Guidelines for Land and Sea Classification" published by China's Ministry of Natural Resources and utilizing the Name and Kind attributes of the POI data, a semantic analysis is conducted to categorize POIs into industrial and non-industrial groups. Subsequently, referring to the "Classification of High-Tech Industries (Manufacturing) (2017)," "Classification of High-Tech Industries (Services) (2018)," and "Classification of Strategic Emerging Industries (2018)" published by the National Bureau of Statistics of China, industrial POIs were further divided into Traditional Industries, High-tech Manufacturing, and High-tech Productive Services (Appendix B).

Furthermore, the VRAD and GHSL datasets are employed in this study to calculate the spatial structure and utilization intensity of parcels. VRAD, developed by a team from Nanjing Normal University, includes Chinese urban building footprints. Meanwhile, the GHSL dataset, created by the European Space Agency using Sentinel-2, Landsat, and global DEM data, is utilized as a tool for assessing human activities on the earth's surface.

2.3 Methodological framework

The methodological framework is divided into five steps, as illustrated in Fig.2.

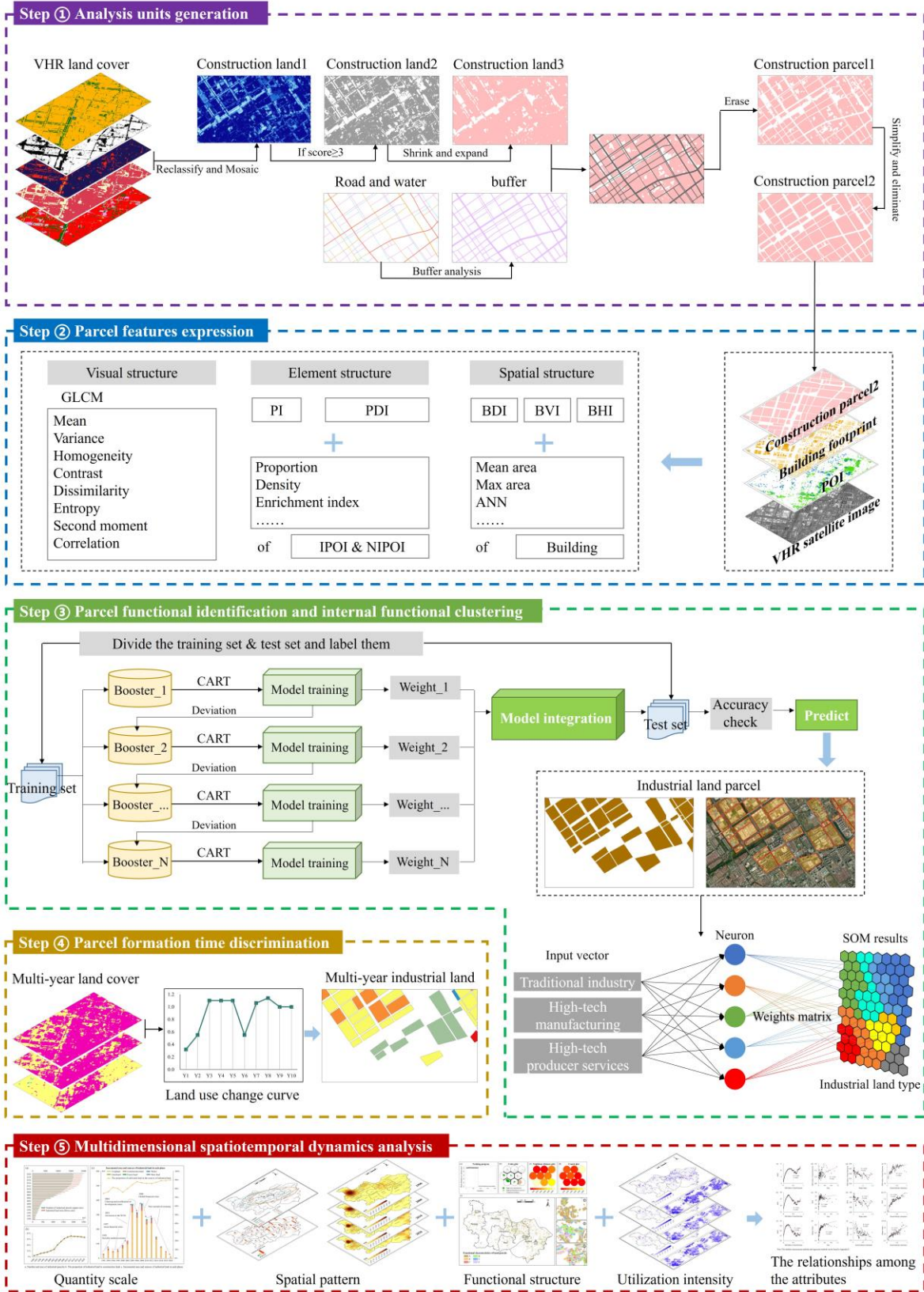
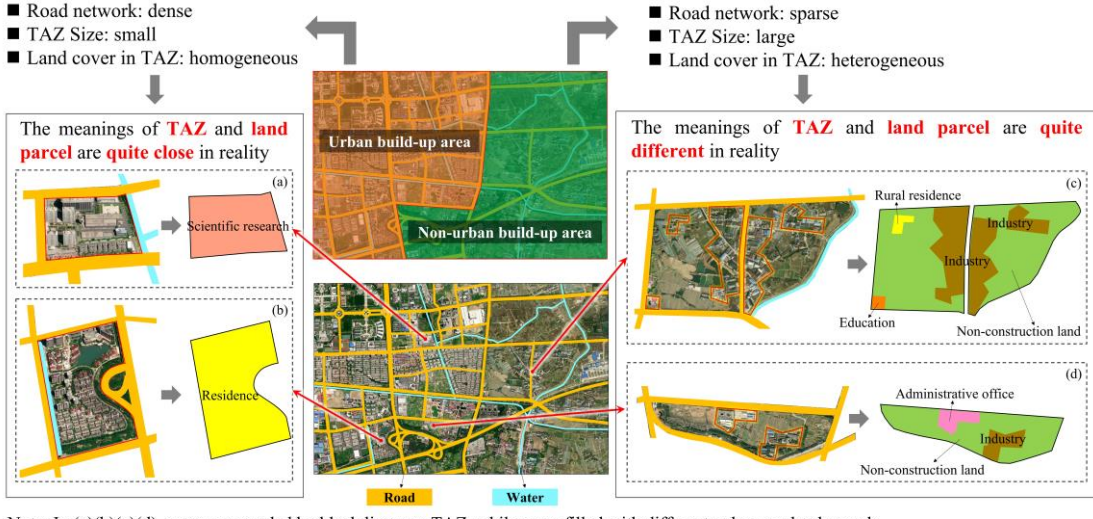


Fig.2. Methodological framework

(1) Analysis unit generation. This step marks a thorough transformation in the method for

generating analysis unit. We move away from the approach used in previous studies, which relied on TAZ as analysis unit, and adopt a parcel-based unit generation method. In previous studies, TAZ was often endowed with the connotation of "urban functional area" (Wu et al., 2023; Zhang et al., 2017) and indeed held significant practical relevance in urban built-up areas with dense road networks (Fig.3a, b). However, industrial land is often found in city peripheries where road networks are sparse and TAZs larger, leading to a higher complexity in land cover (Fig.3c, d). Consequently, using TAZs obscures crucial land details and fails to accurately reflect the functional boundaries within a zone (Qin et al., 2022; Huang et al., 2022a). In response, this study utilizes high-resolution land cover data to extract construction land as matrix elements and employs buffer zones created by linear facilities as dividers (instead of using them to generate TAZs). This adjustment shifts the focus from "functional areas" to more precise "land parcels" (Fig.3c, d), serving three main purposes: Firstly, it refines the granularity of the research, ensuring greater homogeneity in land attributes within each unit. Secondly, it maintains the real-world boundaries, shapes, and sizes, producing parcels that closely mirror actual industrial landforms. Thirdly, it expands the research scope beyond urban centers to encompass suburbs and rural areas, offering a broader and more inclusive analysis.



Note: In (a)(b)(c)(d), areas surrounded by black lines are TAZ, while areas filled with different colors are land parcels

Fig.3. The relationship between "TAZ" and "land parcel "

(2) Parcel features expression. This step focuses on integrating multi-source data including remote sensing images, land cover, POI data, and building information to capture the multidimensional information of the analysis units (land parcels). The information is pivotal for distinguishing industrial land from non-industrial land in Step 3 and for conducting the multidimensional spatiotemporal dynamics analysis of industrial land in Step 5. This study establishes a feature expression framework comprising "visual structure, elemental structure, and spatial structure", and computes 24 feature vectors specifically designed for industrial land (Appendix C). By synthesizing this feature information, this step not only enhances the richness of the data for industrial land identification but also significantly improves accuracy, effectively compensating for the accuracy loss caused by the reliance on single-feature approaches in previous studies. Furthermore, we introduce specific advancements in the computation process, such as adopting the POI efficacy method in place of traditional frequency methods. Unlike approaches that focus solely on the point attributes and frequency characteristics of POI, the POI efficacy method assesses the relationships and relative strengths of POI, ensuring that the

contribution of a particular POI to parcel function identification aligns more closely with its actual societal contribution.

(3) Parcel functional identification and internal functional clustering. This step is dedicated to segregating industrial land parcel from the broader category of construction land using the detailed parcel information derived from Step 2. We implement the ensemble machine learning algorithm, XGBoost, as our predictive model. XGBoost outperforms other models such as Random Forest (RF) by refining the gradient boosting framework and employing regularization techniques to mitigate overfitting. Crucially, XGBoost excels in managing imbalanced datasets through the strategic adjustment of sample weights, thus providing a distinct edge in predicting infrequent categories. After pinpointing industrial land, the analysis proceeds with a Self-Organizing Map (SOM) neural network to delve deeper into the internal functions of such lands, elucidating their usage patterns. As an advanced unsupervised neural network, SOM analyzes input data to create a simplified, discrete representation for effective dimensionality reduction. Diverging from conventional neural networks like Backpropagation (BP) that depend on error correction through backpropagation, SOM adopts a competitive learning approach where neuron competition drives incremental improvements. Consequently, SOM demonstrates robust capabilities in recognizing unfamiliar samples, exhibits considerable resilience against noise, and proves invaluable for clustering and rendering high-dimensional data visually interpretable.

(4) Parcel formation time discrimination. After the identification of industrial land, this study develops an innovative approach known as the Land Use Change Curve Method. This

method is designed to accurately determine the formation time of industrial land, thereby facilitating the compilation of a comprehensive dataset covering the period from 1990 to 2020.

(5) Multidimensional spatiotemporal dynamics analysis of industrial land. In this conclusive step, we formulate a comprehensive framework to analyze both internal and external attributes of industrial land. Utilizing parcel-level data derived from earlier steps, this framework supports a detailed exploration of the complex spatiotemporal dynamics of industrial land within the case study area.

2.4 Analysis unit generation

Firstly, to improve the accuracy of unit generation, this study adopts the "voting" principle to generate the base map of construction land. Land cover types ①-⑤ (Appendix A) are reclassified, assigning a value of 1 to impervious surface and 0 to the rest. The rasters are then summed using ArcGIS's raster calculator, and those with a score of ≥ 3 are selected. Subsequently, construction land rasters are scaled with the operation sequence and number of pixels as: shrink by 2, expand by 4, shrink by 2 again. This step achieves two purposes: one is to remove the adhesion between road and construction land, improving the base map's accuracy, and the other is to fill the voids inside the construction land, enhancing the base map's continuity. After performing the above operations, raster data are vectorized. Next, buffer zones are established for the linear data obtained from OSM. In choosing the linear features, compared to the traditional method of using only road networks, we also incorporate hydrological data, considering the significant impact of the dense water network in the Southern Jiangsu region on land use. Referring to the "Technical Standards for Highway

Engineering" in China, the buffer zone width is set to 70m for motorways, 50m for primary, secondary, tertiary, and trunk roads, 30m for railways, and 20m for water systems. The buffer layer is used to erase the construction land vector layer. Further, land parcels are simplified, voids are eliminated, and the redundant parcels that are too small or lack POIs and buildings are removed. Finally, this process generates a construction land parcel layer for the study area.

2.5 Parcel features expression

This study establishes a feature expression system from three aspects: visual structure, elemental structure, and spatial structure, calculating 24 feature vectors (Appendix C).

Regarding visual structure, the study employs the Gray Level Co-occurrence Matrix (GLCM) in ENVI to calculate eight texture features, including contrast and correlation, from the Landsat images of the study area (Appendix C). These features are then mapped to the parcel level.

In terms of elemental structure, we adopt the POI efficacy method in response to the limitations of the POI frequency method. Based on Equations (1) and (2), the Parcel Function Evaluation Index (PI) and Parcel Function Density Index (PDI) are developed, where higher values suggest a higher likelihood of the parcel being designated as industrial land. Subsequently, inspired by Zhang et al. (2022) and Qin et al. (2022), and considering that Baidu search platform is one of the most popular search engines in China, we utilize web crawling techniques to retrieve Baidu entries for each POI subcategory. The number of search results returned is considered as an indicator of their social influence in the study area. Furthermore, it is then normalized to a range of 0 to 10 as the efficacy score for that category of POIs. When

linking POIs to parcels using ArcGIS, considering that some POIs are situated at the edges of geographical features, such as factory entrances, the following matching rule is applied: a POI is considered to have a location correspondence relationship with a parcel if it falls within the parcel boundaries or within a 15-meter range from the parcel edge. Additionally, traditional indicators commonly used in previous research, such as POI enrichment index, are also retained.

$$PI_i = \sum IP_{ij} \times w_j - \sum NP_{ik} \times w_k \quad (1)$$

$$PDI_i = \frac{PI_i}{A_i} \quad (2)$$

where PI_i is the Function Evaluation Index for parcel i ; PDI_i is the Function Density Evaluation Index for parcel i ; A_i is the area of parcel i ; IP_{ij} is the number of industrial POI of type j on parcel i ; NP_{ik} is the number of non-industrial POI of type k on parcel i ; w_j is the efficacy score for industrial POI of type j ; w_k is the efficacy score for non-industrial POI of type k .

In terms of spatial structure, this study utilizes the GHSL and VRAD dataset to calculate the Building Density Index (BDI), Building Volume Index (BVI), and Building Height Index (BHI) to express the internal spatial utilization morphology of parcels (Equations 3-5). Additionally, traditional metrics such as the average base area of buildings within a parcel, the maximum area, and the average nearest neighbor distance of buildings are retained. These indices collectively offer a nuanced portrayal of the spatial structure within industrial parcels, facilitating a detailed analysis of their spatial utilization patterns.

$$BDI_i = \frac{PBA_i}{PA_i} = \frac{\sum PBA_{ij}}{PA_i} \quad (3)$$

$$BVI_i = \frac{PBV_i}{PA_i} = \frac{\sum PBV_{ij}}{PA_i} \quad (4)$$

$$BHI_i = \frac{BVI_i}{BDI_i} \quad (5)$$

$$BR_i = \frac{BVI_i}{FH_i} \quad (6)$$

where BDI_i is the Building Density Index of parcel i ; BVI_i is the Building Volume Index of parcel i , closely related to the floor-area ratio, and its relationship with the floor-area ratio is represented by Equation 6; BHI_i is the Building Height Index of parcel i ; PBA_i is the sum of the building footprint area on parcel i ; PA_i is the area of parcel i ; PBA_{ij} is the building footprint area on the j^{th} 100×100m grid on parcel i ; PBV_i is the sum of the volume of all buildings on parcel i ; PBV_{ij} is the volume of buildings on the j^{th} 100×100m grid on parcel i ; BR_i is the floor-area ratio of parcel i ; FH_i is the average height of a single floor of buildings on parcel i .

2.6 Parcel functional identification and internal functional clustering

This study employs the XGBoost model for identifying industrial parcels. Nanjing, the capital of Jiangsu Province, is selected as our sample set for training the model. Initially, parcel functions are labeled based on Nanjing's territorial spatial planning annex and remote sensing images to represent the actual ground situation. Subsequently, 80% of the acquired samples are randomly selected as the training set, and 20% as the test set. During training, a model is initialized by XGBoost based on the training set, and the training data are predicted, with residuals calculated for each sample. Subsequently, the gradient boosting algorithm is employed by XGBoost to construct decision trees. The best splitting points are selected through a greedy algorithm, optimizing the objective function. The model progressively enhances its predictive accuracy by minimizing residuals and refining the model's predictions. After 200 iterations, numerous weak classifiers are integrated to form a robust final classifier. The prediction results of each decision tree are weighted and summed up to obtain the prediction

set for the study area.

Afterward, a Self-Organizing Map (SOM) neural network is employed to categorize the internal functional features of the identified industrial land parcels. Subsequently, industrial POIs, having been classified secondarily, are spatially overlaid onto their respective parcels. This process calculates the proportion of each type of industrial POI within each parcel. Subsequently, the processed data is imported into a selected 3×3 hexagonal network. Based on changes in the weight vectors, the number of iterations is adjusted. Through the neural network's autonomous learning, effective clustering of the functional characteristics of the industrial parcels is accomplished.

2.7 Industrial parcel formation time discrimination

By overlaying annual land cover data with the industrial land parcels vector layer, the formation years of industrial parcels are established through Land Use Change Curves, thus obtaining long-term series (1990-2020) industrial land data. First, Equations 7 and 8 are applied to calculate the Land Development Index (LDI) and Relative Land Development Index (RLDI) for each year from 1990 to 2020 within the parcel, where RLDI measures the similarity of land use patterns each year to that at the end of the study period. Subsequently, land use change curves for each parcel are generated based on RLDI. Based on these curves, industrial land formation pathways can be categorized into four types: a) One-time Development, b) Progressive Development, c) Non-industrial Construction Land Conversion, and d) Industrial Land Upgrading. Fig.4 elaborates on the RLDI curve characteristics, real-world implications, and time determination markers for each type of industrial land parcel. Finally, by comparing

and analyzing the Land Use Change Curves of manually marked parcels in the sample set, the time determination markers for the four types of industrial parcels are defined. Based on this tool, the formation years of all parcels are determined. One-time and Progressive Development types of industrial lands are determined based on $RLDI \geq 0.8$ and $RLDI \geq 0.6$, respectively, at the time point of industrial land formation. The Conversion type is determined based on the secondary formation time point during the rising phase of the land use change curve. The Upgrading type is determined based on the initial formation time point of the parcel before the decline phase in the Land Use Change Curves.

$$LDI_{ij} = \frac{Con_{ij}}{Area_i} \quad (7)$$

$$RLDI_{ij} = \frac{LDI_{ij}}{LDI_{i2020}} \quad (8)$$

where LDI_{ij} is the Land Development Index for parcel i in year j ; Con_{ij} is the area of construction land within parcel i in year j ; $Area_i$ is the area of parcel i ; LDI_{i2020} is the Land Development Index for parcel i at the end of the study period in 2020; $RLDI_{ij}$ is the Relative Land Development Index, which, in cases c and d, may exceed 1.

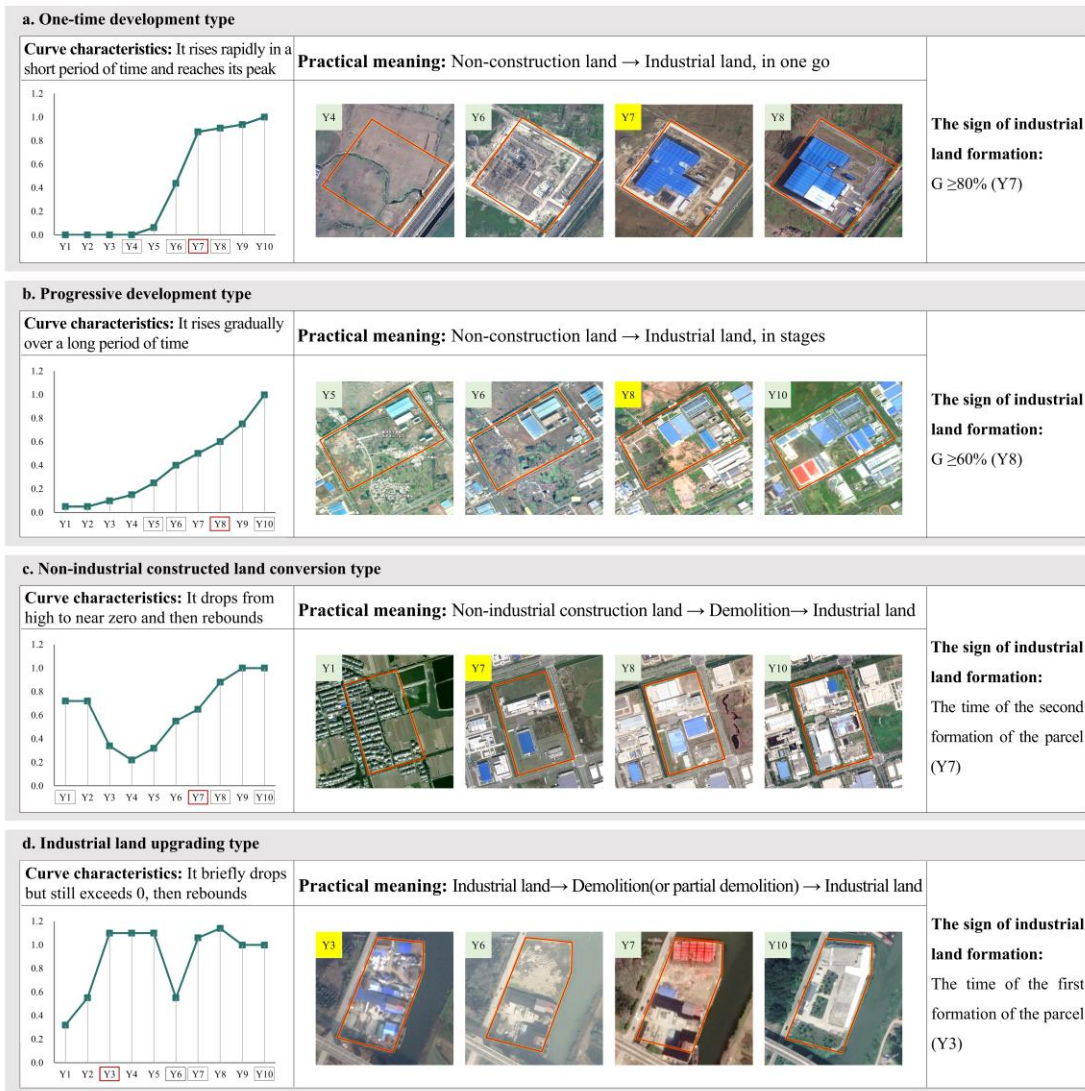


Fig.4. Discrimination of the formation time of industrial land

2.8 Multidimensional spatiotemporal dynamics analysis for industrial land

To systematically analyze the spatiotemporal dynamics of industrial land, we propose a multidimensional analysis framework that covers two levels (internal and external) and four dimensions (quantity scale, spatial pattern, functional structure, utilization intensity) of industrial land's key attributes (Fig.5). In external attributes, the quantity scale attribute, which is the most basic external characteristic of industrial land (Kuang et al., 2016), is represented by the number of parcels, area, and conversion sources. The spatial pattern attribute reflects the geographical location and interrelations of industrial land (Tan et al., 2024), characterized

through spatial distribution features, spatial agglomeration characteristics, and spatial growth patterns. Within the internal attributes, the functional structure highlights industrial diversity and upgrade potential (Long, 2022; Huang et al., 2022a), determined by clustering in section 2.5 and quantified with metrics like the Shannon Diversity Index. Utilization intensity, reflecting the manner and efficiency of internal space utilization, is determined by BDI, BVI, and BHI calculated in section 2.5.

The study employs a suite of specific methods, such as overlay analysis, Standard Deviation Ellipse (SDE), Kernel Density Estimation (KDE), buffer analysis, Local Moran'I, and regression analysis. A detailed exposition of these methods and their applications is provided in Appendix D.

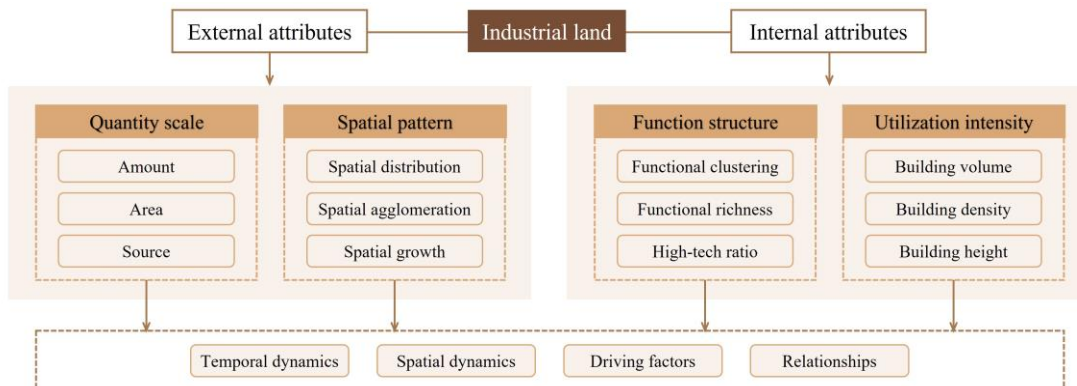


Fig.5. Multidimensional spatiotemporal dynamics analysis framework of industrial land

3. Results

3.1 Identification results and accuracy verification of industrial land parcels

Following the established technical pathway, a total of 16,067 industrial parcels are identified within the Southern Jiangsu Urban Agglomeration over the period from 1990 to 2020. Fig.6 illustrates the geometric morphology, spatial layout, and formation times of these industrial land parcels. By zooming on three typical industrial areas, it is evident that the boundaries and shape features of the parcels are expressed in considerable detail.

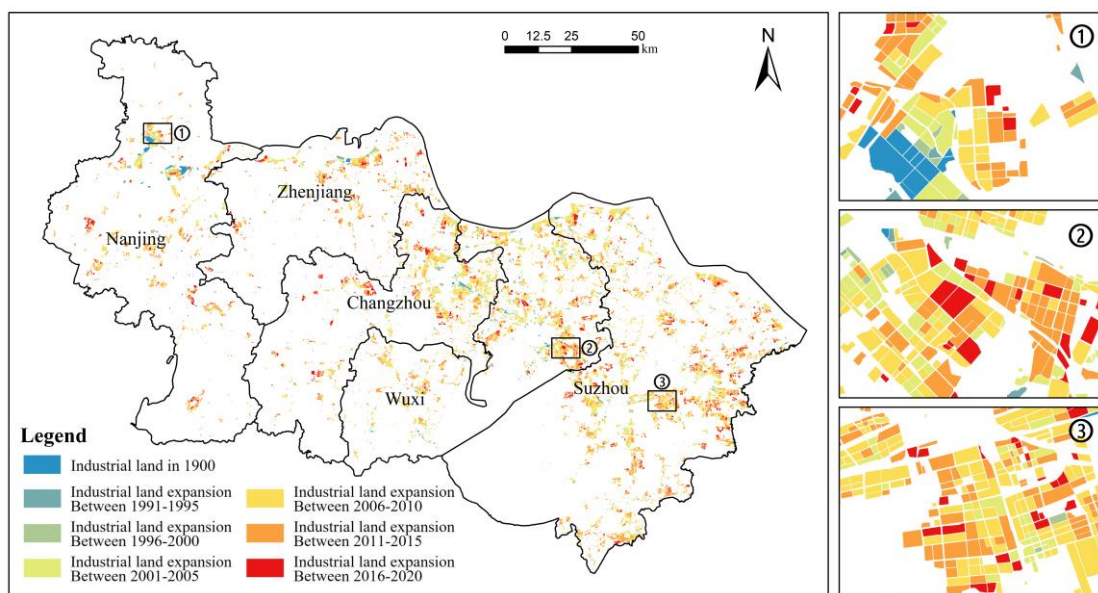


Fig.6. Industrial land parcels in the study area

In the process of testing the accuracy of industrial land identification and temporal discrimination, the accuracy for the test set is automatically calculated through the results of the machine learning model. Meanwhile, the entire dataset of the study area is assessed by comparing identified samples against actual land use situations. The original materials used for the accuracy tests include Landsat and historical remote sensing images from Google Earth.

Accuracy testing for industrial land identification involves randomly selecting 300 parcels within the study area, including both industrial and non-industrial land parcels. The

identification results of these parcels are compared with historical remote sensing imagery to verify consistency with actual land use. During the manual verification process, criteria for determining parcels that mix industrial and non-industrial uses (such as residential and educational) are established. If the classification aligns with the predominant functional use within the parcel, it is deemed correctly identified; otherwise, it is considered incorrectly identified. Ultimately, a confusion matrix is generated, and three metrics are calculated: overall accuracy (OA), producer's accuracy (PA), and user's accuracy (UA). The test results demonstrate high accuracy and stability for industrial land identification (Table 1 and Fig.7a). Results show that both PA and UA are closely matched and exceed 85% for both the test set and the entire dataset. With an OA of 94.70% for the test set and 91.33% for the complete dataset (Table 1), the model exhibits exceptional performance in identifying industrial land.

Table 1 Accuracy test of industrial land identification

	PA	UA	OA
Test set	88.04%	88.52%	94.70%
Entire set	86.96%	85.11%	91.33%

In terms of accuracy testing for parcel time discrimination, 300 industrial parcels are selected annually and compared with historical remote sensing imagery to verify the accuracy of determining the parcels' formation years. During the testing process, a one-year margin of error is permitted. For instance, if a parcel was actually developed in 2013, a determination within the range from 2012 to 2014 is deemed accurate. The accuracy of parcel time determination using the Land Use Change Curve method is 82.63%. Analyzing the data by period (Fig.7b), except for 1990, where the accuracy is slightly higher due to the inclusion of all industrial lands formed before this year, the accuracy for other years generally shows a

progressive improvement. This result may be attributed to the increased precision of the original data used to generate the Land Use Change Curves.

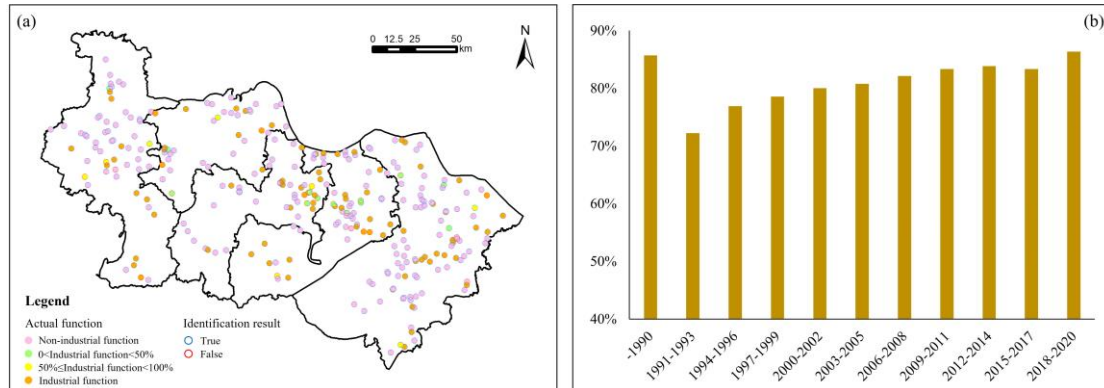


Fig.7. Accuracy test results of industrial land identification and temporal discrimination

3.2 Spatiotemporal dynamics of external attributes

3.2.1 Quantity scale of industrial land

(1) Characteristics of Quantity Scale

The area of industrial land has consistently expanded, increasing from 107.61 km² in 1990 to 2431.56 km² in 2020, which represents a more than a twentyfold increase (Fig.8a). The single-period increment exhibits an "inverted U-shaped" evolution characteristic, with the period from 2003 to 2012 marking the rapid growth phase. During this decade, the expansion in industrial land constituted 70.09% of the total increase observed over the entire study period (Fig.8c). Using 2002 and 2012 as dividing points, the proportion of industrial land in construction land underwent three phases: slow increase, rapid increase, and slow decrease, peaking at 40.44% in 2012 (Fig.8b). This indicates that prior to 2012, the expansion of industrial land in the Southern Jiangsu Urban Agglomeration outpaced that of other types of construction land. However, post-2012, there was a noticeable adjustment in the composition of construction land growth, shifting away from a predominant focus on industrial use.

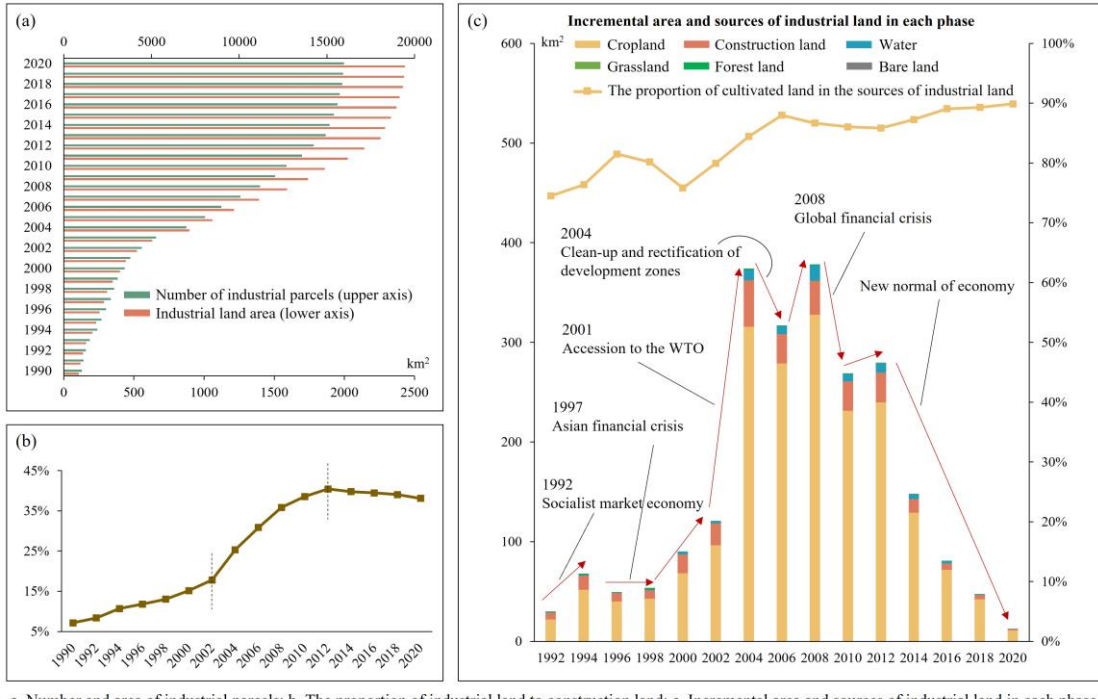


Fig.8. Industrial land scale change and expansion sources

(2) Sources of industrial land

Fig.8c illustrates that farmland, existing construction land, and water bodies are the three primary sources of industrial land growth. Among these, farmland is the dominant source, and its proportion showing a trend of continuous increase. Additionally, among the three natural land types of forest, grassland, and water, industrial land expansion has encroached the most on water. This indicates a common practice of "land reclamation from water" in the water-rich Southern Jiangsu Urban Agglomeration. These findings suggest that the expansion of industrial land in the study area poses a significant threat to farmland and ecological conservation.

3.2.2 Spatial pattern of industrial land

(1) Spatial distribution characteristics

During the study period, the centroid of industrial land distribution shifted southeastward, leading to a spatial imbalance characterized by a higher concentration in the southeast and a

lower concentration in the northwest. As demonstrated in Fig.9a, between 1990 and 2010, the center of the SDE for industrial land distribution moved 58.15km in a southeastward direction, exacerbating spatial imbalances. In the southeastern region, 21 districts accounted for 77.28% of the total industrial land area (Fig.9b). Between 2010 and 2020, there was no significant movement in the center of the standard deviation ellipse, but the area of the ellipse increased by 8.53%, indicating that industrial land growth during this period tended towards a broader range and lower density.

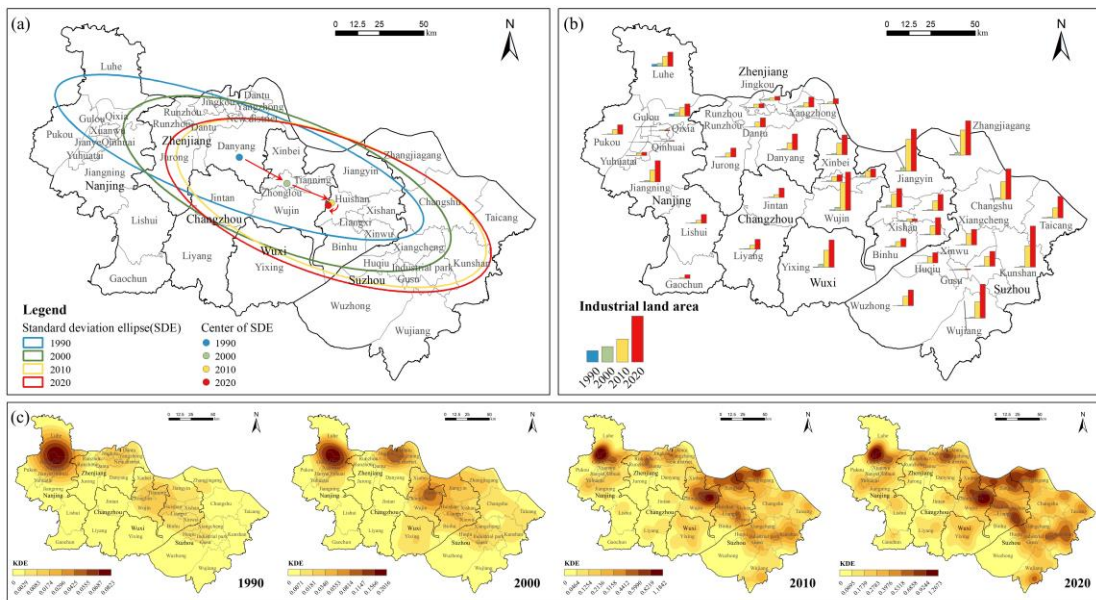


Fig.9. Spatial pattern of industrial land and its evolution

(2) Spatial agglomeration characteristics

The agglomeration of industrial land evolved from single-center to multi-centers, and then towards the integration into hotspot regions. KDE analysis depicted in Fig.9c illustrates that the emergence and movement of industrial land aggregation hotspots mirror to the characteristics of industrial land spatial distribution. Between 1990 and 2010, the main changes in industrial land agglomeration were evidenced by an increase in the number of hot cores and

the expansion of their range. From 2010 to 2020, changes in the agglomeration pattern of industrial land were not significant, but the strength of the already formed hot cores continued to increase. The boundaries of some hot cores in the southeastern part of the study area began to merge, significantly enhancing the spatial correlation of industrial land use.

(3) Spatial growth characteristics

Four spatial growth patterns of industrial land are identified: Outward Expansion, Inward Infill, Strip Extension, and Mixed Growth (Fig.10).

Outward Expansion Type. This pattern is characterized by dispersive expansion around the original urban built-up area, serving as the primary industrial land growth mode in the study area. A typical example is the industrial land evolution process in Kunshan (Fig.10a), where earlier-formed industrial land are closer to the city center, and more recently formed ones are further away. Surface graph analysis indicates that the center of industrial land growth in this area is located within rings at distances of 5km, 6km, 8km, 9km, and 9km from the city center over time, showing clear characteristics of outward expansion.

Inward Infill Type. This pattern is manifested by initially forming an encircling shape of industrial land around a region and gradually filling towards the center (Fig.10b). Such spatial evolution patterns often appear in government-planned new industrial zones with a short history of construction, like the Suzhou Industrial Park and Nanjing Qixia District, which were established in the 1990s.

Strip Extension Type. This pattern is primarily characterized by the expansion of industrial

land along or perpendicular to transportation lines. In the Southern Jiangsu Urban Agglomeration, the primary transportation lines that facilitate such development include the Yangtze River and key railways, such as the influence of the Yangtze River shoreline on the industrial land evolution process in Jiangyin (Fig.10c).

Mixed Growth Type. In addition to these three patterns, some areas exhibit mixed spatial evolution characteristics influenced by various factors. Taking Changzhou as an example (Fig 10d), the city is traversed by a railway and surrounded by relatively open terrain. As a result, industrial land gradually expands away from the city center and perpendicular to the railway line, demonstrating mixed growth characteristics.

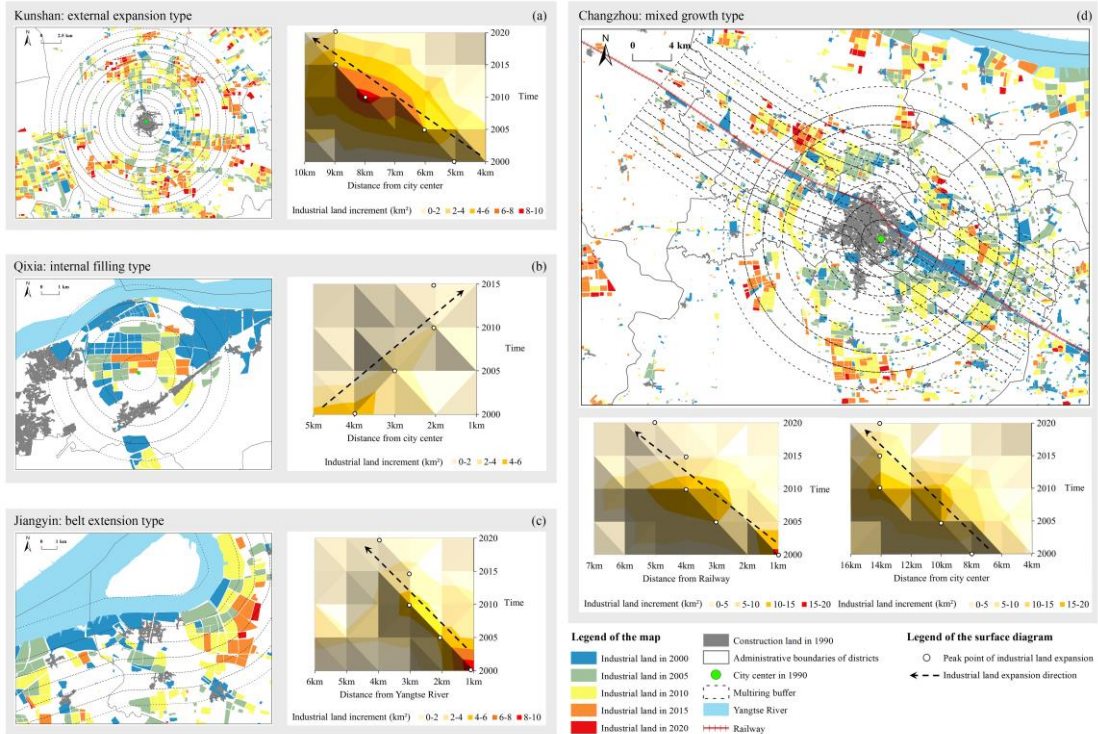


Fig.10. Spatial growth patterns of industrial land

3.3 Spatiotemporal dynamics of internal attributes

3.3.1 Functional structure of industrial land

Fig.11a demonstrates that during the training of the SOM network for the internal functional clustering of industrial land, the weight vector exhibits a significant reduction at 800 iterations, signaling well-optimized weights between neurons. When integrating insights from Fig.11b, Fig.11c, and Fig.11d, it is evident that the map produced after 2000 iterations includes 9 neurons. Neurons positioned at the upper part are predominantly influenced by traditional industries, possess a numerical superiority, and feature shorter neighboring distances, which reflects a more homogenous functional structure among these industrial parcels. Conversely, neurons located at the lower part are chiefly dominated by high-tech industries. These are markedly less in quantity and exhibit larger neighboring distances, suggesting a diverse structure and more flexible land use practices. The central area serves as a transition zone, characterized by units with extensive functional intermixing. Subsequent repeated experiments determine that categorizing neurons into six groups optimizes homogeneity within each group and enhances distinctions among them (Fig.11b). The functional characteristics of industrial land are categorized as follows: Traditional Industry Dominated (A), High-Tech Manufacturing Dominated (B), High-Tech Productive Services Dominated (C), Mixed High-Tech Manufacturing and Traditional Industry (D), Mixed High-Tech Productive Services and Traditional Industry (E), and Highly Mixed Functions (F). The visualization of the functional characteristics of industrial lands in the study area is shown in Fig.11e.

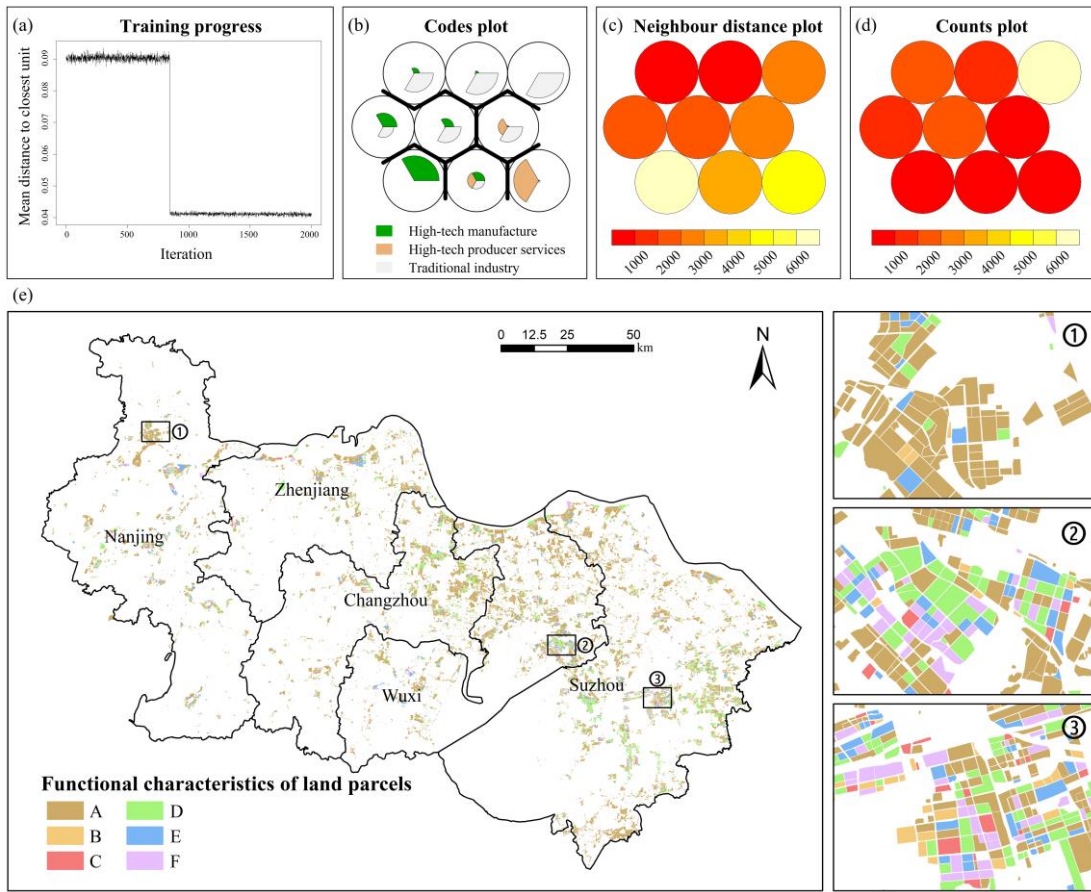


Fig.11. Clustering results of SOM on functional characteristics of industrial land

From the perspective of the scale of each type (Fig.12a), Traditional Industry Dominated land parcels have consistently been the main type at every stage. The proportion of the five categories involving high-tech industries initially shows a trend of declining, then rising and eventually stabilizing. This pattern indicates that in the Southern Jiangsu Urban Agglomeration, the growth of the high-tech industry has led to the transformation of industrial land structure from single-function to multi-functional. High-tech industrial land hotspots have exhibited a trend towards the southeastern part (Fig.12b), aligning with the overall movement of industrial land distribution hotspots. However, the distinction lies in the fact that high-tech industrial land hot cores are more concentrated, indicating that such high-tech enterprises exhibit a higher degree of aggregation and more intensive land use.

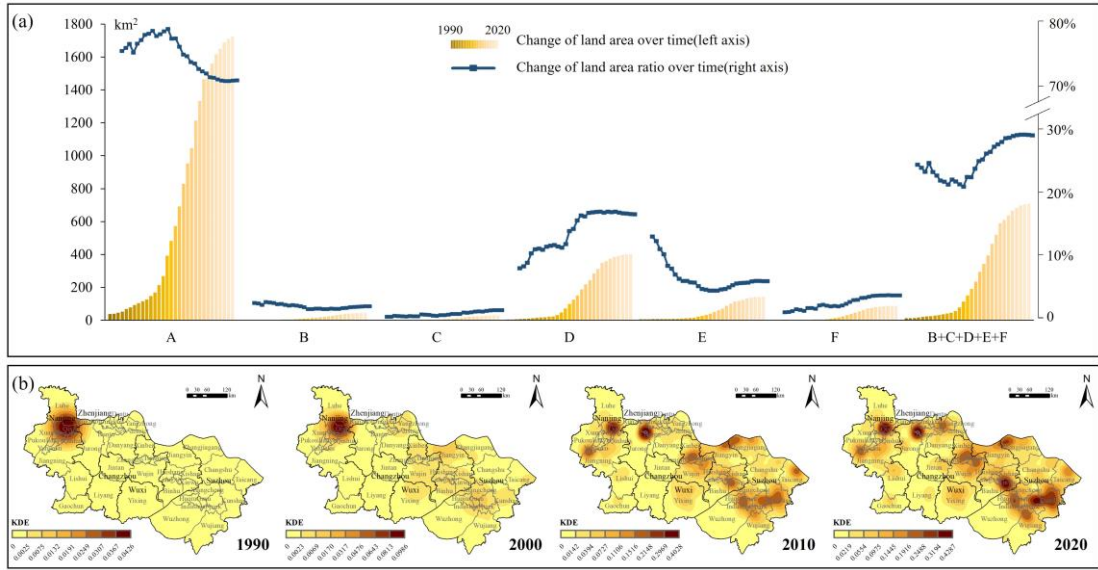


Fig.12. Evolution of function structure of industrial land

3.3.2 Utilization intensity of industrial land

Appendix E presents the calculation results for each industrial parcel's Building Density Index (BDI), Building Height Index (BHI), and Building Volume Index (BVI). Given that BVI most comprehensively reflects the construction intensity of parcels, the analysis primarily focuses on this index.

The utilization intensity of industrial land underwent a "U-shaped" process of initially declining and then increasing during the study period (Fig.13a). The utilization intensity experienced two phases of decline between 1990-1995 and 2000-2005, and began to increase after 2005, with the rate of increase moderating after an initial rapid growth. Moreover, the high-value areas of industrial land utilization intensity gradually spread from the central urban areas to the surrounding counties (Fig.13b-h). In 2000, the northern part of Nanjing and the central urban areas of Suzhou-Wuxi-Changzhou exhibited higher industrial land utilization intensities. However, after 2010, counties outside the central urban areas, such as Huishan

Wuzhong (Fig.13g and h), saw significant improvements in industrial land utilization intensity. This indicates a clear diffusion effect of industrial land utilization intensity, where advanced industrial areas have catalyzed the development of industrial clusters and enhanced land use efficiency through spatial spillover effects.

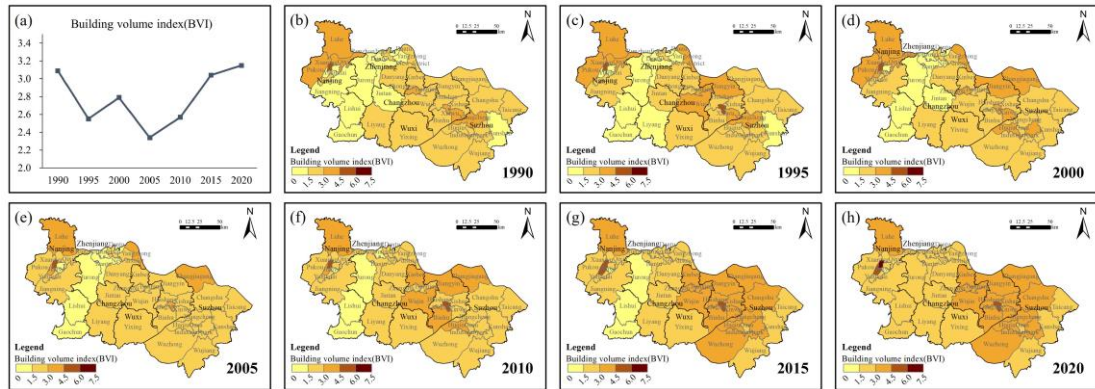


Fig.13. Evolution of utilization intensity of industrial land

3.4 Correlation among different attributes of industrial land

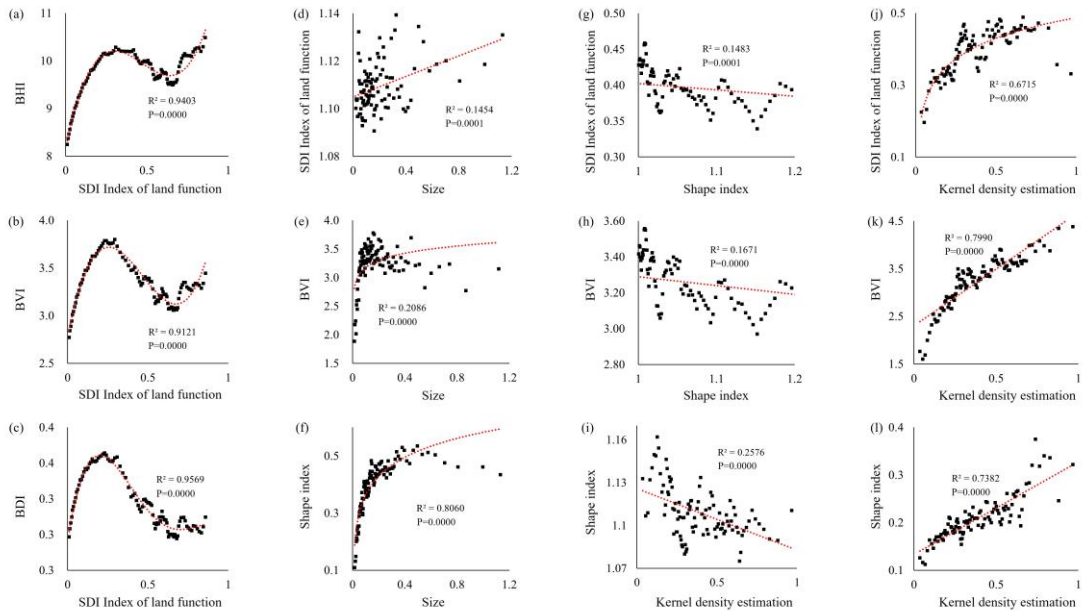
Parcel-level data also supports further analysis of the correlation among different attributes of industrial land.

Firstly, the building height and building volume of industrial land parcels exhibit an "N-shaped" relationship with the richness of parcel functions, while the building density displays an "inverted U-shaped" relationship with the same (Fig.14a-c). This suggests that land parcels with a mix of functions are planned and constructed with a larger proportion of green spaces, roads, and other non-building facilities, opting not to pursue the densification of buildings. Instead, they enhance utilization intensity mainly by increasing construction height, reflecting a land use approach that values three-dimensional space more.

Secondly, the richness of functions, utilization intensity, and shape complexity all show a positive relationship with land parcel size (Fig.14d-f), while the richness of functions and

utilization intensity have a negative relationship with shape complexity (Fig.14g&h). This indicates that industrial parcels with high utilization intensity and richness of functions tend to be accompanied by larger land area and more regular parcel shapes.

Lastly, in terms of the relationship between spatial patterns and other attributes (Fig.14 i, j, k, l), parcels in industrial agglomerations, compared to scattered lands, have advantages in terms of function mixing, land intensity, parcel size, and shape regularity. Additionally, calculating the Local Moran'I Index further verified the spatial autocorrelation of these attributes in industrial land (Appendix F).



Note: The attribute measurement methods and regression methods can be found in Appendix E.

Fig.14. The relationships among the attributes of industrial land

4. Discussion

4.1 Performance of industrial land identification method and the impact of different strategies

This study develops a yearly pathway for identifying industrial land parcels based on multi-source data. The scope of the study encompasses both urban and rural industrial land, addressing the shortcomings of existing research, which often overlook comprehensive urban-rural considerations. On this expanded basis, the models also achieve superior accuracy. The overall accuracy of our industrial land identification is 94.70%, representing an improvement of 6.5% and 11.98% over the studies by Zhong et al. (2020) and Su et al. (2023), respectively; The producer's accuracy is 88.04%, marking an increase of 18.84% and 25.04% compared to Zhang et al. (2020) and Li et al. (2022), respectively; The user's accuracy is 88.52%, which is a 13.52% improvement over Zhang et al. (2020) and is close to the accuracy reported by Li et al. (2022). This indicates improvements in all three aspects of industrial land identification accuracy by our method, particularly contributing to the producer's accuracy. It means that a large number of industrial land parcels were previously misclassified as other land types in previous studies, and our technological pathway successfully identified these overlooked industrial parcels. Although the training samples in this paper are selected from one city, the model trained on this sample achieves performance close to the prediction set across the entire study area, proving our training model's strong portability.

Moreover, this study effectively categorizes the functional features of industrial land into six categories using the SOM network. Through detailed analysis of each type's functional structure, the credibility of the clustering results is confirmed. In Types A, B, and C, dominated

by a single function, the primary type of enterprise constitutes 93%, 98%, and 91% of enterprises on the parcels, respectively. Type D, featuring Mixed High-Tech Manufacturing and Traditional Industry, shows a balanced distribution of enterprise types. Type E, featuring Mixed High-Tech Productive Services and Traditional Industry, shows a significant disparity in the distribution of enterprise types, with enterprises accounting for 33% and 61% respectively. However, these figures align with China's "Guidelines for the Implementation of Industrial Land Policies", which restrict service-oriented building areas to no more than 30% of a project's total area. Lastly, Type F, characterized by Highly Mixed Functions, has an almost even distribution among three enterprise types at 33%, 32%, and 34%.

4.1.1 Impact of unit generation method

Previous studies generally utilized TAZ as the analysis unit for land function identification, while this paper innovatively employs a parcel-based unit generation method. Fig.15 clearly illustrates the differences in unit generation results between the two methods. It's evident that due to the lack of clear boundaries between construction land and non-construction land in OSM data, the generated TAZs fail to adhere to the principle that analysis unit should ensure homogeneity of land use characteristics, leading to mismatches between the analysis unit and the actual land use pattern (Fig.15b and d). Conversely, the analysis unit generated using the "parcel-based method" in this study align more closely with the actual land use status in terms of land area, shape, and boundary lines (Fig.15c and e), thus effectively improving the accuracy of industrial land identification.

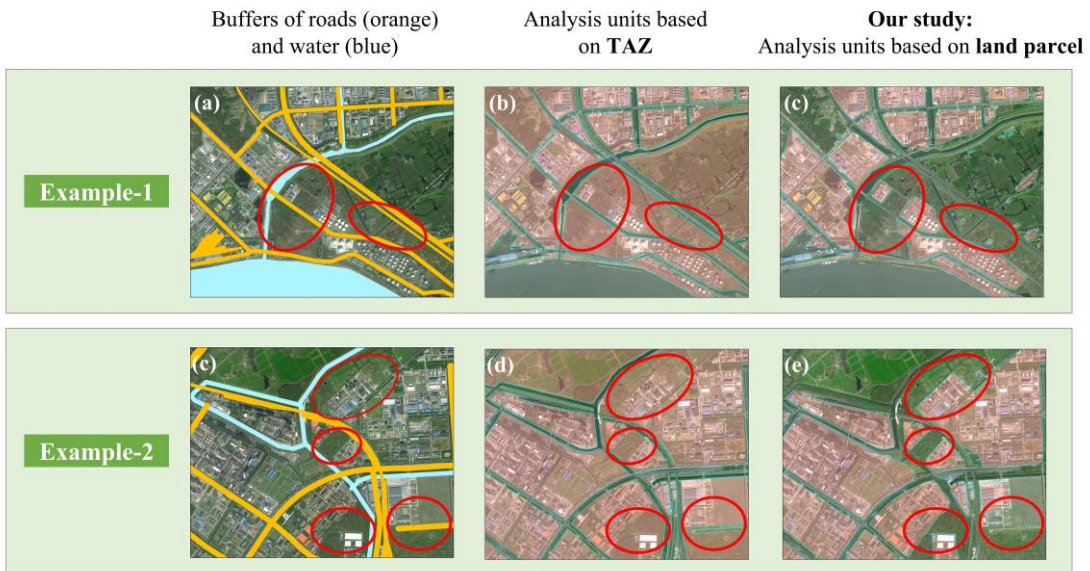


Fig.15. Comparison of unit generation results using "TAZ method" and "parcel-based method"

4.1.2 Impact of features expression method

The performance of different features expression methods on the accuracy of industrial land identification is compared (Table 2). From the perspective of single-type features, the elemental structure (E) performs the best, while the visual structure (V) performs the worst. However, if traditional indicators such as the frequency of various types of POI alone are used to represent the elemental structure (E*), both producer's accuracy and user's accuracy decrease by more than 10% compared to the performance of E. This indicates that developing the Parcel Function Evaluation Index (PI) and Parcel Function Density Index (PDI) as supplements to the expression method of elemental structure is necessary and effective. In terms of combined features, the V+E+S combination used in this study performs the best, where the elemental structure (E) and spatial structure (S) contribute significantly to identification accuracy, and the inclusion of visual structure (V) leads to a slight improvement. This finding also reaffirms that relying solely on visual features presented on the earth's surface for land function identification, especially when using only remote sensing imagery data, results in extremely unstable

judgment outcomes. Given that many innovative enterprises today do not exhibit the typical visual features seen in traditional industrial factories, relying solely on visual features easily leads to misclassification. Therefore, conducting research through a method integrating multi-source data is essential.

Table 2 Comparison of identification accuracy of different features expression method

	UA	PA	OA
Visual structure (V)	58.50%	47.61%	80.05%
Element structure (E)	76.71%	77.35%	89.72%
E*	63.61%	65.62%	84.54%
Spatial structure (S)	62.85%	52.08%	82.82%
V+E	78.02%	80.39%	90.58%
V+S	71.47%	67.13%	86.70%
E+S	85.22%	81.67%	92.80%
V+E*+S	80.83%	84.10%	92.36%
V+E+S (Our study)	88.52%	88.04%	94.70%

E* refers to the element structure after removing the Parcel Function Evaluation Index (PI) and Parcel Function Density Index (PDI) developed in this study.

4.1.3 Impact of machine learning models

A comparison of commonly used machine learning models shows that the three ensemble learning models (XGBoost, RF, Adaboost) outperform single models (DT, SVM) (Table 3). The XGBoost model used in our study achieved the best accuracy results in all three aspects of industrial land identification. Additionally, the closest alignment between UA and PA was observed with XGBoost and Adaboost. This indicates that the Boosting ensemble algorithms, compared to the Bagging ensemble algorithm (such as RF), provide more stable performance when dealing with unbalanced samples. They more effectively address the issue of imbalance between UA and PA as evidenced in prior studies by Lu et al. (2022) and Wu et al. (2023).

Table 3 Comparison of identification accuracy of different machine learning models

Model	UA	PA	OA
XGBoost (Our study)	88.52%	88.04%	94.70%
RF	87.32%	85.44%	93.84%
Adaboost	84.64%	83.70%	92.98%
DT	86.05%	81.77%	91.44%
SVM	85.36%	78.03%	91.38%

4.2 Applicability and implications

This study develops a new technical pathway and analytical framework, demonstrating their potential applicability in industrial land studies. The analysis based on this framework holds significant theoretical importance for elucidating the multidimensional spatiotemporal dynamics of industrial land, and it provides valuable insights for the sustainable use and refined management of industrial land in practice.

4.2.1 Evolution direction, intensity, and speed of industrial land

This study reveals the evolution direction, intensity, and speed of various dimensional attributes of industrial land over 30 years, analyzed at both the parcel and administrative district levels. The integrated analysis across various dimensions demonstrates that the evolution speed of industrial land exhibits an "inverted U-shaped" pattern, where it accelerates initially and then decelerates. As it approaches the late stage of industrialization, the attributes across dimensions gradually stabilize, and the marginal contribution of new land to the transformation of industrial land diminishes (Appendix G). These conclusions align with related research findings (Xie et al., 2019; Wang et al., 2020), but our analysis deepens these by embracing multi-dimensional assessments rather than single-dimensional ones. Moreover, the study identifies that the evolution of different attributes is not synchronous but exhibits significant variances. Specifically, in the case area, the external attributes (quantity scale and spatial

pattern) and internal attributes (functional structure and utilization intensity) of industrial land reached turning points around 2010 and 2015, respectively, highlighting a lag of approximately five years in the transformation of internal attributes behind external attributes (Appendix G). Furthermore, the implication for policymakers is that the focus of industrial land management in the region ought to shift from external expansion to enhancing the intrinsic qualities of existing land. This entails exploring the internal utilization intensity and upgrading spatial functions to boost land use efficiency and mitigate risks to food and ecological security (Fig.8).

4.2.2 Spatial association and differentiation of industrial land

Spatial analysis based on parcel-scale data allows for a more detailed revelation of spatial patterns. Firstly, the results indicate significant spatial autocorrelation in industrial land use, with industrial parcels in close spatial proximity exhibiting similar dimensional attributes (Appendix H), aligning with the first law of geography. Moreover, the spatial association of industrial land strengthens as the industrialization process evolves, with hotspot areas of industrial land distribution gradually converging (Fig.9). The spatial spillover effects of industrial lands in central city areas continue to emerge. (Fig.13). Additionally, the spatial heterogeneity in industrial land use is very pronounced, highlighting the importance of tailoring land policies to local conditions. For example, in this case study area, the evolution speed of the attributes of industrial lands in the southeastern part of the urban agglomeration is faster, significantly surpassing those in the west in terms of scale, utilization intensity, and functional complexity. This conclusion reveals potential areas for industrial land renewal, particularly emphasizing the transformation of industrial land in the western part of the study area.

4.2.3 Interrelations among different attributes of industrial land

In the process of industrial land use, various attributes do not evolve and function independently. Compared to single-dimensional analysis, a multi-dimensional framework-based study reveals interlinkages between different attributes (Fig.14). This interlinkage effect specifically manifests in the complex associations between external and internal attributes of industrial land, and these associations may be nonlinear. For instance, the "inverted U-shaped" relationship between building density and the richness of parcel functions, and the "N-shape" relationship between building volume and the richness of parcel functions, as discovered in this study. Revealing these interrelations not only deepens our understanding of industrial land dynamics but also offers insights for directing its utilization, suggesting that focusing solely on changes in one attribute during industrial land transformation could considerably reduce the effectiveness of such interventions. Therefore, planning is expected to take into account compatibility among various attributes. For instance, when transitioning the function of industrial land from traditional industry to high-tech industry, greater flexibility in terms of mixed-use functions, floor area ratio, etc., need to be considered to align with the land characteristics of the target industry.

4.2.4 The interaction between the spatiotemporal dynamics of industrial land and other factors

Although this study does not employ mathematical models to analyze the driving factors behind the spatiotemporal dynamics of industrial land, it offers a framework for analysis and tools for gathering baseline data on this topic. Furthermore, by comparing the findings of this study with key economic and policy milestones in the study area (see Appendix H and

Appendix I), potential interactions between the spatiotemporal dynamics of industrial land and these factors can still be observed.

The role of economic factors is first manifested in their strong coupling with changes in the scale of industrial land. Over 70% of the industrial lands in the Southern Jiangsu Urban Agglomeration were developed between 2003 and 2012 (Fig.8c), a period that aligns closely with the era of rapid industrial economic growth. During this time, the annual growth rate of industrial value added exceeded 15% in most years (Appendix H). Additionally, the spatial evolution of industrial land is also significantly influenced by economic factors. The transformation of industrial land in the southeastern part of the study area has notable advantages over the northwest (Fig.9, Fig.12, and Fig.13), primarily due to the geographic benefits of its coastal location (especially proximity to Shanghai), which facilitates participation in global industrial trade (Zhuang & Ye, 2020). Lastly, the impact of sudden economic events on the spatiotemporal dynamics of industrial land cannot be overlooked. Notable incidents such as the 1997 Asian financial crisis and the 2008 global financial crisis prompted discernible fluctuations in the evolution of industrial land within the following 1-2 years (Fig.8, Fig.12).

The interaction between policy factors and land use has always captivated researchers. This study elucidates how the evolution of both internal and external attributes of industrial land is intricately linked with current policies, highlighting the government's pivotal role in the allocation and utilization of industrial land (Appendix I). A deeper analysis reveals intriguing findings. For instance, post-2010, there was a marked trend towards large-scale, low-density

expansion of industrial land in the northwestern part of the study area, evidenced by the movement of Standard Deviation Ellipses in the opposite direction of the general trend. These phenomena, which do not align with the high-tech industry's preference for clustered site selection (see Figs.12 and 14), may reflect higher-level government interventions aimed at mitigating spatial inequalities in industrial development by artificially directing the allocation of industrial land towards the northwest. However, the efficacy of this policy intervention merits further examination. Local Moran's I analysis from 2015 to 2020 indicates significant addition of industrial parcels with Low-Low (LL) clustering in terms of utilization intensity in the northwestern area (Appendix F). In contrast, there is no obvious LL clustering in the southeast, despite the larger scale of new industrial land there. This disparity suggests pronounced spatial heterogeneity in the attractiveness of newly added industrial lands to businesses, while highlighting a spatial mismatch where scarce land resources are not fully utilized. The land disproportionately allocated to the northwest has not been fully utilized. From a policy perspective, this indicates that excessive government intervention may lead to suboptimal resource allocation, highlighting the need for caution.

4.3 Limitations and research prospects

While significant progress has been made in our study on the relevant topics, there remain some potential limitations. In terms of industrial land identification, labeling training samples requires considerable manual effort and high-quality initial data. Future research could explore integrating the methods described in this paper with unsupervised classification models to achieve semi-automatic or fully automatic labeling. Additionally, building on the multi-dimensional attribute analysis framework for industrial land parcels developed in this study,

future research and land use planning decisions could further refine the types of industries within the internal function analysis of parcels as needed. This refinement would facilitate a sector-specific exploration of their land use characteristics, providing more nuanced insights to guide practical decision-making.

5. Conclusion

This study innovatively develops a methodological framework based on the integration of multi-source data for analyzing the multidimensional spatiotemporal dynamics of industrial land. It has been successfully applied to a case study of the Southern Jiangsu Urban Agglomeration spanning from 1990 to 2020.

Upon evaluation, industrial land identification accuracy significantly outperforms existing methods, achieving overall accuracy, producer's accuracy, and user's accuracy at 94.70%, 88.04%, and 88.52% respectively, with temporal discrimination accuracy at 82.63%. The parcel morphology faithfully mirrors actual parcel boundaries, shapes, and areas. Moreover, the analytical framework effectively addresses two levels (internal and external) and four dimensions (quantity and scale, spatial pattern, functional structure, intensity of use) of industrial land attributes. This framework proves its applicability in long-term time series analysis and in encompassing both urban and rural settings. The study highlights the framework's capability to analyze the direction, intensity, and speed of industrial land attributes' evolution, and to expose spatial associations and differentiations in industrial usage. It also elucidates interrelations among attributes and offers insights into the interactions between the spatiotemporal dynamics of industrial land and various factors, providing a robust method for collecting baseline data.

The industrial land area in the study region expanded dramatically from 107.61 km² to 2431.56 km², revealing an imbalanced spatial distribution with higher concentration in the southeast compared to the northwest. Over time, spatial agglomeration transitioned from a

single-center to a multi-center configuration, eventually forming hotspot areas. Spatial growth exhibited four distinct patterns: Outward Expansion, Inward Infilling, Strip Extension, and Mixed Growth. Concurrently, the functional structure of industrial land evolved from single to composite functions and gradually stabilized. Initially, the intensity of industrial land use decreased, then increased, with high-value areas progressively extending from the central urban areas to surrounding counties. There is a significant correlation among different industrial land attributes and spatial autocorrelation within the same attributes. The transformation speed of various attributes follows an "inverted U-shaped" trajectory during the study period. Notably, the evolution of internal attributes lags behind external attributes by approximately five years, with the southeast experiencing faster changes than the northwest. Socioeconomic and policy factors are crucial in driving the evolution of industrial land.

This study provides new insights and methods for analyzing the detailed dynamics of industrial land in large-scale study areas, and offers practical implications for the sustainable use and management of industrial land.

References

- Chen, W., Chen, W., Ning, S., Liu, E.-n., Zhou, X., Wang, Y., & Zhao, M. (2019). Exploring the industrial land use efficiency of China's resource-based cities. *Cities*, 93, 215-223.
- Dai, D., Yang, J., & Rao, Y. (2022). Spatial-temporal evolution of industrial land transformation effect in eastern China. *Frontiers in Environmental Science*, 10.
- Fang, F., Zeng, L., Li, S., Zheng, D., Zhang, J., Liu, Y., & Wan, B. (2022). Spatial context-aware method for urban land use classification using street view images. *ISPRS Journal of Photogrammetry and Remote Sensing*, 192, 1-12.
- Gao, J., Qiao, W., Ji, Q., Yu, C., Sun, J., & Ma, Z. (2021). Intensive-use-oriented identification and optimization of industrial land readjustment during transformation and development: A case study of Huai'an, China. *Habitat International*, 118.
- Gao, Y., & Ma, Y. (2015). What is absent from the current monitoring: Idleness of rural

industrial land in suburban Shanghai. *Habitat International*, 49, 138-147.

Gu, Z., Jin, X., Liang, X., Liu, J., Han, B., & Zhou, Y. (2024). Diversification of food production in rapidly urbanizing areas of China, evidence from southern Jiangsu. *Sustainable Cities and Society*, 101.

He, Q., & Tang, X. (2022). Identification and Analysis of Industrial Land in China Based on the Point of Interest Data and Random Forest Model. *Frontiers in Environmental Science*, 10.

Huang, C., Xiao, C., & Rong, L. (2022a). Integrating Point-of-Interest Density and Spatial Heterogeneity to Identify Urban Functional Areas. *Remote Sensing*, 14(17).

Huang, L., Xiang, S., & Zheng, J. (2022b). Fine-Scale Monitoring of Industrial Land and Its Intra-Structure Using Remote Sensing Images and POIs in the Hangzhou Bay Urban Agglomeration, China. *International Journal of Environmental Research and Public Health*, 20(1).

Ilieva, R. T., & McPhearson, T. (2018). Social-media data for urban sustainability. *Nature Sustainability*, 1(10), 553-565.

Jiang, G., Ma, W., Dingyang, Z., Qinglei, Z., & Ruijuan, Z. (2017). Agglomeration or dispersion? Industrial land-use pattern and its impacts in rural areas from China's township and village enterprises perspective. *Journal of Cleaner Production*, 159, 207-219.

Jiang, H. (2021). Spatial-temporal differences of industrial land use efficiency and its influencing factors for China's central region: Analyzed by SBM model. *Environmental Technology & Innovation*, 22.

Kuang, W., Liu, J., Dong, J., Chi, W., & Zhang, C. (2016). The rapid and massive urban and industrial land expansions in China between 1990 and 2010: A CLUD-based analysis of their trajectories, patterns, and drivers. *Landscape and Urban Planning*, 145, 21-33.

Li, C., Gao, X., He, B.-J., Wu, J., & Wu, K. (2019). Coupling Coordination Relationships between Urban-industrial Land Use Efficiency and Accessibility of Highway Networks: Evidence from Beijing-Tianjin-Hebei Urban Agglomeration, China. *Sustainability*, 11(5).

Li, D., Yang, L., Lin, J., & Wu, J. (2020). How industrial landscape affects the regional industrial economy: A spatial heterogeneity framework. *Habitat International*, 100.

Li, Q., Chen, W., Li, M., Yu, Q., & Wang, Y. (2022). Identifying the effects of industrial land expansion on PM2.5 concentrations: A spatiotemporal analysis in China. *Ecological Indicators*, 141.

Li, X., Zhang, C., & Li, W. (2017). Building block level urban land-use information retrieval based on Google Street View images. *GIScience & Remote Sensing*, 54(6), 819-835.

Liang, X., Zhao, T., & Biljecki, F. (2023). Revealing spatio-temporal evolution of urban visual environments with street view imagery. *Landscape and Urban Planning*, 237.

Long, H. (2022). Theorizing land use transitions: A human geography perspective. *Habitat International*, 128.

Lu, W., Tao, C., Li, H., Qi, J., & Li, Y. (2022). A unified deep learning framework for urban functional zone extraction based on multi-source heterogeneous data. *Remote Sensing of Environment*, 270.

Luo, N., Wan, T., Hao, H., & Lu, Q. (2019). Fusing High-Spatial-Resolution Remotely Sensed Imagery and OpenStreetMap Data for Land Cover Classification Over Urban Areas. *Remote Sensing*, 11(1).

- Mao, L., Zheng, Z., Meng, X., Zhou, Y., Zhao, P., Yang, Z., & Long, Y. (2022). Large-scale automatic identification of urban vacant land using semantic segmentation of high-resolution remote sensing images. *Landscape and Urban Planning*, 222.
- Nie, W., Fan, X., Nie, G., Li, H., & Xia, C. (2022). Building Function Type Identification Using Mobile Signaling Data Based on a Machine Learning Method. *Remote Sensing*, 14(19).
- Niu, H., & Silva, E. A. (2023). Understanding temporal and spatial patterns of urban activities across demographic groups through geotagged social media data. *Computers, Environment and Urban Systems*, 100.
- Park, J.-I., & Kim, J.-O. (2022). Does industrial land sprawl matter in land productivity? A case study of industrial parks of South Korea. *Journal of Cleaner Production*, 334.
- Ponce-Lopez, R., & Ferreira, J. (2021). Identifying and characterizing popular non-work destinations by clustering cellphone and point-of-interest data. *Cities*, 113.
- Qiao, L., Huang, H., & Tian, Y. (2019). The Identification and Use Efficiency Evaluation of Urban Industrial Land Based on Multi-Source Data. *Sustainability*, 11(21).
- Qin, Q., Xu, S., Du, M., & Li, S. (2022). Identifying urban functional zones by capturing multi-spatial distribution patterns of points of interest. *International Journal of Digital Earth*, 15(1), 2468-2494.
- Shu, H., & Xiong, P.-p. (2019). Reallocation planning of urban industrial land for structure optimization and emission reduction: A practical analysis of urban agglomeration in China's Yangtze River Delta. *Land Use Policy*, 81, 604-623.
- Su, Y., Zhong, Y., Liu, Y., & Zheng, Z. (2023). A graph-based framework to integrate semantic object/land-use relationships for urban land-use mapping with case studies of Chinese cities. *International Journal of Geographical Information Science*, 37(7), 1582-1614.
- Sun, Y., Ma, A., Su, H., Su, S., Chen, F., Wang, W., & Weng, M. (2020). Does the establishment of development zones really improve industrial land use efficiency? Implications for China's high-quality development policy. *Land Use Policy*, 90.
- Tan, X., Chen, W., Cao, H., Li, Q., & Zhang, S. (2024). Identifying spatiotemporal characteristics and driving factors of industrial land use morphology in China. *Expert Systems with Applications*, 235.
- Tian, L. (2015). Land use dynamics driven by rural industrialization and land finance in the peri-urban areas of China: "The examples of Jiangyin and Shunde". *Land Use Policy*, 45, 117-127.
- Wang, B., Zhang, Y., Zhan, C., & Yang, X. (2020). Strategic interaction of industrial land conveyance behaviors in China: Based on an asymmetric two-regime Spatial Durbin Model. *Journal of Cleaner Production*, 270.
- Wu, H., Luo, W., Lin, A., Hao, F., Olteanu-Raimond, A.-M., Liu, L., & Li, Y. (2023). SALT: A multifeature ensemble learning framework for mapping urban functional zones from VGI data and VHR images. *Computers, Environment and Urban Systems*, 100.
- Xie, H., Chen, Q., Lu, F., Wu, Q., & Wang, W. (2019). Spatial-temporal disparities, saving potential and influential factors of industrial land use efficiency: A case study in urban agglomeration in the middle reaches of the Yangtze River. *Land Use Policy*, 75, 518-529.
- Xie, H., Zhai, Q., Wang, W., Yu, J., Lu, F., & Chen, Q. (2018). Does intensive land use promote a reduction in carbon emissions? Evidence from the Chinese industrial sector. *Resources, Conservation and Recycling*, 137, 167-176.

Xiong, C., Lu, J., & Niu, F. (2020). Urban Industrial Land Expansion and Its Influencing Factors in Shunde: 1995–2017. *Complexity*, 2020, 1-12.

Xu, M., & Zhang, Z. (2021). Spatial differentiation characteristics and driving mechanism of rural-industrial Land transition: A case study of Beijing-Tianjin-Hebei region, China. *Land Use Policy*, 102.

Xu, N., Luo, J., Wu, T., Dong, W., Liu, W., & Zhou, N. (2021). Identification and Portrait of Urban Functional Zones Based on Multisource Heterogeneous Data and Ensemble Learning. *Remote Sensing*, 13(3).

Yan, X., Tuo, H., & Lai, Y. (2022). A Two-Way Fixed Effects Estimation on the Impact of Industrial Land Supply on Environmental Pollution in Urban China. *Int J Environ Res Public Health*, 19(22).

Yang, J., Tang, W., Gong, J., Shi, R., Zheng, M., & Dai, Y. (2023). Simulating urban expansion using cellular automata model with spatiotemporally explicit representation of urban demand. *Landscape and Urban Planning*, 231.

Yap, M. D., Nijensteijn, S., & van Oort, N. (2018). Improving predictions of public transport usage during disturbances based on smart card data. *Transport Policy*, 61, 84-95.

Yin, G., Lin, Z., Jiang, X., Qiu, M., & Sun, J. (2020). How do the industrial land use intensity and dominant industries guide the urban land use? Evidences from 19 industrial land categories in ten cities of China. *Sustainable Cities and Society*, 53.

Yuan, J., Wang, S., Wu, C., & Xu, Y. (2022). Fine-Grained Classification of Urban Functional Zones and Landscape Pattern Analysis Using Hyperspectral Satellite Imagery: A Case Study of Wuhan. *IEEE Journal of Selected Topics in Applied Earth Observations and Remote Sensing*, 15, 3972-3991.

Yue, L., Miao, J., Ahmad, F., Draz, M. U., Guan, H., Chandio, A. A., & Abid, N. (2022). Investigating the role of international industrial transfer and technology spillovers on industrial land production efficiency: Fresh evidence based on Directional Distance Functions for Chinese provinces. *Journal of Cleaner Production*, 340.

Zhai, W., Bai, X., Shi, Y., Han, Y., Peng, Z.-R., & Gu, C. (2019). Beyond Word2vec: An approach for urban functional region extraction and identification by combining Place2vec and POIs. *Computers, Environment and Urban Systems*, 74, 1-12.

Zhang, J., Zhang, D., Huang, L., Wen, H., Zhao, G., & Zhan, D. (2019). Spatial distribution and influential factors of industrial land productivity in China's rapid urbanization. *Journal of Cleaner Production*, 234, 1287-1295.

Zhang, L., Yue, W., Liu, Y., Fan, P., & Wei, Y. D. (2018). Suburban industrial land development in transitional China: Spatial restructuring and determinants. *Cities*, 78, 96-107.

Zhang, N., Zhang, J., Chen, W., & Su, J. (2022). Block-based variations in the impact of characteristics of urban functional zones on the urban heat island effect: A case study of Beijing. *Sustainable Cities and Society*, 76.

Zhang, W., Li, W., Zhang, C., Hanink, D. M., Li, X., & Wang, W. (2017). Parcel-based urban land use classification in megacity using airborne LiDAR, high resolution orthoimagery, and Google Street View. *Computers, Environment and Urban Systems*, 64, 215-228.

Zhang, X., Du, S., & Wang, Q. (2017). Hierarchical semantic cognition for urban functional zones with VHR satellite images and POI data. *ISPRS Journal of Photogrammetry and Remote Sensing*, 132, 170-184.

Zhang, X., Du, S., & Zheng, Z. (2020). Heuristic sample learning for complex urban scenes: Application to urban functional-zone mapping with VHR images and POI data. *ISPRS Journal of Photogrammetry and Remote Sensing*, 161, 1-12.

Zhong, Y., Su, Y., Wu, S., Zheng, Z., Zhao, J., Ma, A., Zhu, Q., Ye, R., Li, X., Pellikka, P., & Zhang, L. (2020). Open-source data-driven urban land-use mapping integrating point-line-polygon semantic objects: A case study of Chinese cities. *Remote Sensing of Environment*, 247.

Zhou, W., Ming, D., Lv, X., Zhou, K., Bao, H., & Hong, Z. (2020). SO-CNN based urban functional zone fine division with VHR remote sensing image. *Remote Sensing of Environment*, 236.

Zhu, F., Zhang, F., & Ke, X. (2018). Rural industrial restructuring in China's metropolitan suburbs: Evidence from the land use transition of rural enterprises in suburban Beijing. *Land Use Policy*, 74, 121-129.

Zhu, Wang, & Sakai. (2019). Remote Sensing-Based Analysis of Landscape Pattern Evolution in Industrial Rural Areas: A Case of Southern Jiangsu, China. *Sustainability*, 11(18).

Zhuang, L., & Ye, C. (2020). Changing imbalance: Spatial production of national high-tech industrial development zones in China (1988-2018). *Land Use Policy*, 94.

List of Appendices

Appendix A. Data

Appendix B. Industry type division

Appendix C. Parcel features expression measure index

Appendix D. The application of specific methods

Appendix E. BDI (a), BVI (b) and BHI (c) of industrial land (2020 as an example)

Appendix F. Local Moran'I analysis

Appendix G. Comparison of evolution speed of industrial land attributes in different periods

Appendix H. Growth rate of industrial added value in Southern Jiangsu Urban Agglomeration

Appendix I. Related policies/events

Appendix A. Data

Data	Sources	Description	Time
High-resolution remote sensing imagery	Landsat	Raster (30m)	1990-2020
	① ESA_WorldCover	Raster (10m)	2020
	② Cross-Resolution Land-Cover(CRLC)	Raster (10m)	2020
High-resolution land cover	③ FROM_GLC10	Raster (10m)	2017
	④ ESRI_Land_Cover	Raster (10m)	2020
	⑤ SinoLC-1	Raster (1m)	2020
	⑥ China Land Cover Dataset (CLUD)	Raster (30m)	1985-2020
POI	AMAP(https://ditu.amap.com/)	Vector	2020
	NavInfo(https://www.navinfo.com/)	Vector	2020
Road + Water	OpenStreetMap (OSM)	Vector	2020
Building information	Global Human Settlement Layer (GHSL)	raster(10m/100m)	1990-2020
	Vectorized rooftop area data (VRAD)	Vector	2020

Appendix B. Industry type division

Type	Trade
① Traditional industry	Mining industry; Electricity, heat, gas, and water production and supply industry; Other manufacturing industries, excluding②
② High-tech manufacturing	Pharmaceutical manufacturing; Aerospace equipment and apparatus manufacturing; Electronics and telecommunications equipment manufacturing; Computer and office equipment manufacturing; Medical instruments and apparatus manufacturing
③ High-tech producer services	Information chemical product manufacturing; Information transmission, software, and information technology services; Scientific research and technical services

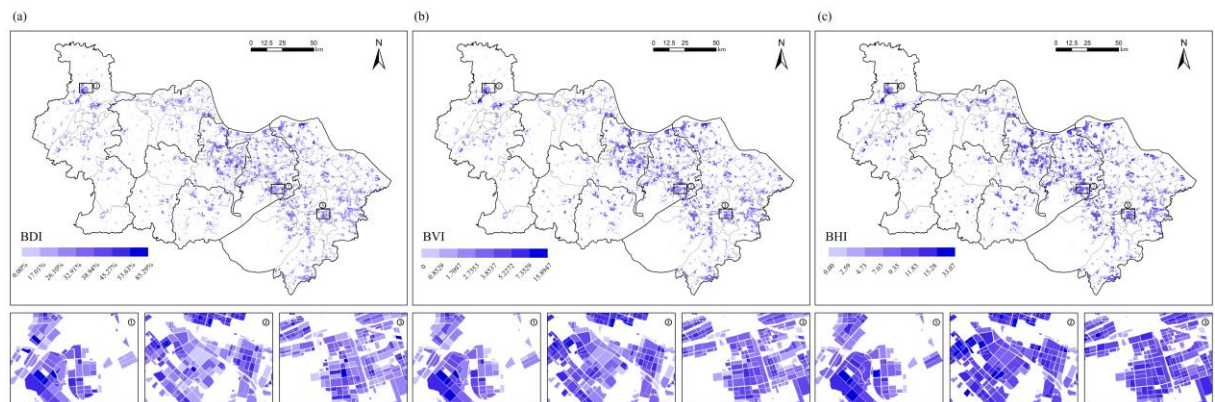
Appendix C. Parcel features expression index

Visual structure	Element structure	Spatial structure
Mean	Parcel function evaluation index (PI)	Building density index (BDI)
Variance	Parcel functional evaluation density index (PDI)	Building volume index (BVI)
Homogeneity	Proportion of industrial POI	Building height index (BHI)
Contrast	Proportion of non-industrial POI	Average base area of building
Dissimilarity	Density industrial of POI	Maximum base area of building
Entropy	Density of non-industrial POI density	Average nearest neighbors of buildings
Second moment	Enrichment index of industrial POI	
Correlation	Enrichment index of non-industrial POI Number of industrial POI Number index of non-industrial POI	

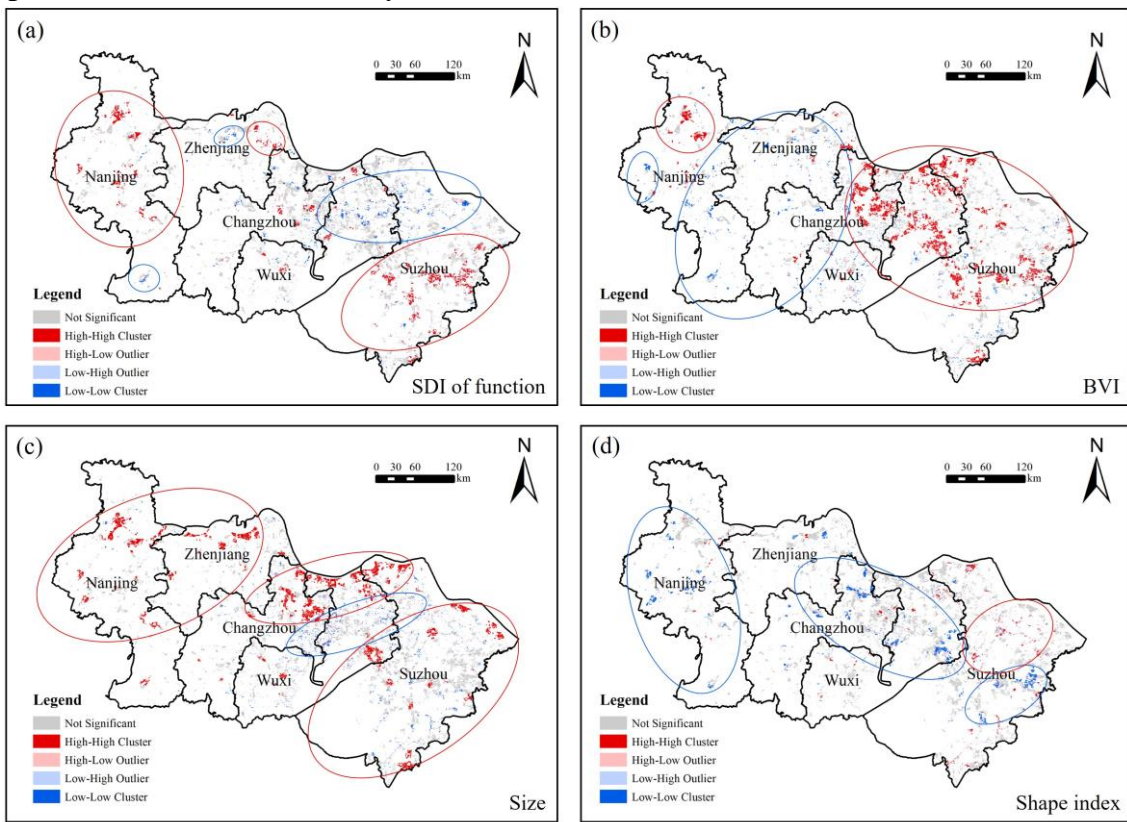
Appendix D. The application of specific methods

Methods	Application
Standard Deviation Ellipse (SDE)	Utilized to analyze the spatial distribution and evolutionary characteristics of industrial lands. The SDE quantitatively delineates overall features like centrality, dispersion, directionality, and spatial morphology using parameters such as the center, major axis, minor axis, and orientation angle.
Kernel Density Estimation (KDE)	Implemented in phases with parcel area as the weight, KDE generates grayscale maps. Results are categorized into eight levels using the Natural Breaks method (Jenks), with the top three levels designated as hotspots. This method is critical for analyzing spatial clustering and evolution of industrial land.
Buffer analysis	This method analyzes spatial growth patterns of industrial land hotspots up to 2020. Starting with the urban built-up area boundary from 1990, multi-ring buffer zones are developed using ArcGIS based on the built-up area center and main transportation lines, with buffer widths adjusted according to the industrial land hotspot size. This analysis helps explore formation processes and spatial path differences of industrial land agglomerations.
Regression analysis	Regression analysis is employed to examine the relationships among five attributes of industrial parcels: size, spatial location, function richness, utilization intensity, and shape complexity. Here's a breakdown of the process: (1) Data Collection: Attributes for 16,067 parcels are quantified. Parcel size is determined by area, spatial location by industrial land distribution kernel density zoning statistics, function richness by the Shannon Diversity Index of parcel functions, utilization intensity by BVI, BDI, and BHI, and shape complexity by the Shape Index. (2) Data Sorting and Preparation: Parcels are first sorted by the measure value of the independent variable from smallest to largest. A sliding window of 1000 units is then used to compute the sliding average for the dependent variable. For regression analysis, 100 data sets are selected using the equal interval method. (3) Regression Analysis: This step involves performing regression on the variables, including log transformations or adding squared terms to uncover non-linear relationships.
Local Moran'I	Using ArcGIS's "Cluster and Outlier Analysis" tool, Local Moran's I assesses spatial autocorrelation in four attributes: parcel size, functional richness, utilization intensity, and shape complexity. Results are categorized into distinct groups such as High-High clustering (HH) and Low-Low clustering (LL), among others.

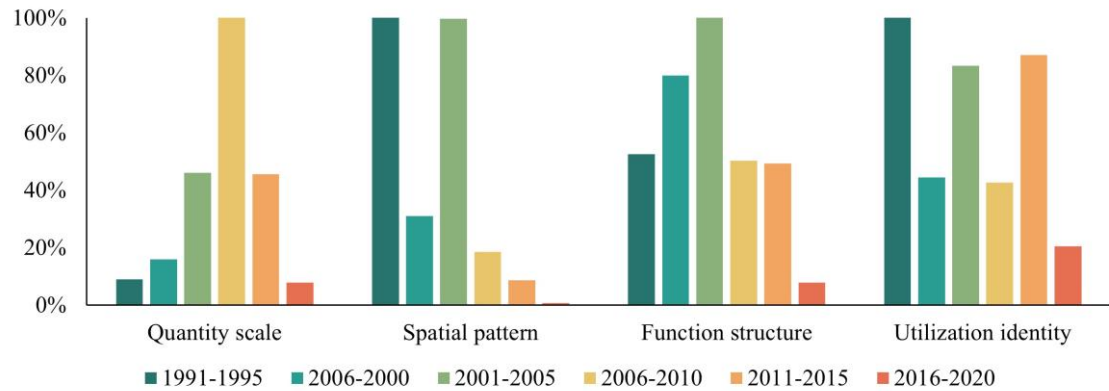
Appendix E. BDI (a), BVI (b) and BHI (c) of industrial land (2020 as an example)



Appendix F. Local Moran's I analysis



Appendix G. Comparison of evolution speed of industrial land attributes in different periods



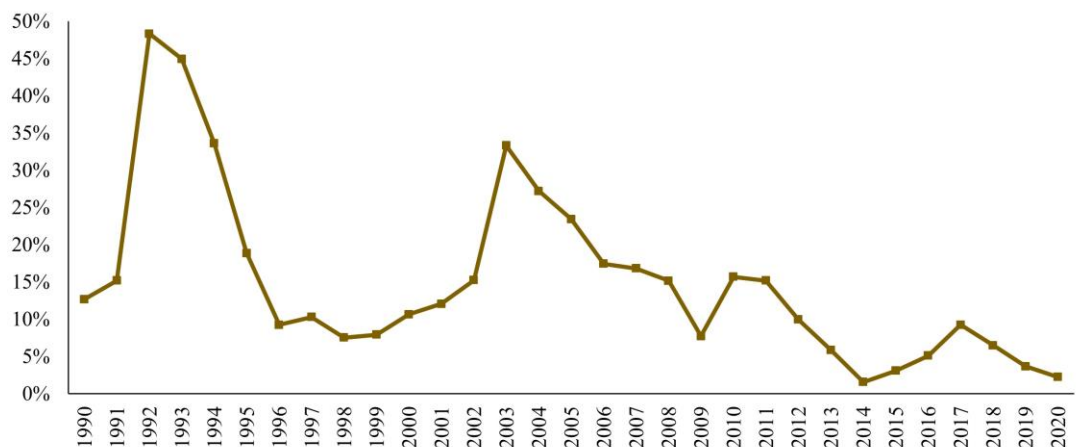
Caption:

Rate of Change Formula:

$$r_i = \frac{|x_i - x_{i-1}|}{\max|x_i - x_{i-1}|}$$

Where: r_i is the relative rate of change of the attribute in period i ; x_i is the value of the attribute in period i ; x_{i-1} is the value of the attribute in period $i - 1$. The quantity scale is represented by the proportion of industrial land to construction land, the spatial pattern is represented by the movement distance of the center of the standard deviation ellipse, the function structure is represented by the Shannon Diversity Index (SDI) of parcel function, and utilization identity is represented by the Building Volume Index (BVI).

Appendix H. Growth rate of industrial added value in Southern Jiangsu Urban Agglomeration



Appendix I. Related policies/events

Time	Related policies/events
1992	Establishment of China's socialist market economy.
1997	Asian Financial Crisis.
2001	China's accession to the WTO.
2003	Notice on Clearing and Rectifying Various Development Zones and Strengthening Construction Land Management has been issued. Comprehensive rectification of inefficient development zones initiated by the Chinese government.
2004	Decision of the State Council on Deepening Reform and Strict Land Management issued. Clarification that increased plot ratios per planning requirements incur no additional land use fees.
2006	Notice of the State Council on Strengthening Land Regulation and Related Issues was issued, mandating that industrial land must be sold through bidding, auction, and listing methods. This marked the first time the Chinese government stipulated such a requirement, effectively enhancing the marketization level of land supply.
2008	Global financial crisis.
2011	Implementation of the Outline of the 12th Five Year Plan for Land and Resources. Launch of land conservation evaluations in development zones to promote intensive and economical land use, strengthening of land use planning and annual planning control, significant reduction in the supply of industrial land.

Innovative framework for identification and spatiotemporal dynamics analysis of industrial land at parcel scale with multidimensional attributes

Weilong Kong ^a, Jing Huang ^a, Lu Niu ^a, Shuocun Chen ^a, Jiahe Zhou ^a, Zhengfeng Zhang ^{a,*}

a School of Public Administration and Policy, Renmin University of China, Beijing, 100872, People's Republic of China

***Corresponding author: Zhengfeng Zhang**

Tel: +86-010-82502296

E-mail: zhangzhengfeng@ruc.edu.cn

Address: Room 403 Qiushi Building, Renmin University of China,
Zhongguancundajie Road, Haidian District, Beijing, 100872, PR
China

Declaration of Interest Statement: There are no conflicts of interest to declare.